https://doi.org/10.5194/essd-2022-44
Preprint. Discussion started: 17 February 2022

Open Access Earth System Science Data Discussions

Ice Surface Velocity in the Eastern Arctic from Historical Satellite SAR Data

Tazio Strozzi[1], Andreas Wiesmann[1], Andreas Kääb[2], Thomas Schellenberger[2] and Frank Paul[3]

[1]Gamma Remote Sensing, 3073 Gümligen, Switzerland
[2]Department of Geosciences, University of Oslo, 0316 Oslo, Norway
[3]Department of Geography, University of Zurich, 8057 Zürich, Switzerland

Correspondence to: Tazio Strozzi (strozzi@gamma-rs.ch)

Abstract. Knowledge on ice surface velocity of glaciers and ice caps contributes to a better understanding of a wide range of processes related to glacier dynamics, mass change and response to climate. Based on the recent release of historical SAR data from various space agencies we compiled nearly complete mosaics of winter ice surface velocities for the 1990's over the Eastern Arctic (Novaya Zemlya, Franz-Josef-Land, Severnaya Zemlya and Svalbard), a region with sparse optical velocity records from these years. We mainly applied offset-tracking to JERS-1 SAR data and filled data gaps using SAR interferometry and offset-tracking from ERS-1/2 SAR data. We studied the long-term variability of winter ice surface velocity by comparing our 1990's results to 2008-2011 velocity maps from ALOS-1 PALSAR-1 and 2020-2021 maps from Sentinel-1. A general increase of winter velocities from the 1990's to present along with a retreat of glacier fronts is obsverved. Exceptions to this general pattern are surges, which are widespread over Svalbard but rarely found in the other three regions. The dense time series of ice surface velocity from Sentinel-1 since 2015 were also considered to infer the representativeness of winter data with respect to mean annual values. We found that for non-surging glaciers short-term seasonal fluctuations are relatively small and winter ice surface velocities are a good representative of mean annual velocities with an underestimation of less than 10%. Together with consistent datasets of glacier ice thickness and terminus position, the ice surface velocities in the Eastern Arctic provide the basis to quantify the regional decadal average calving flux during the 1990's. The ice surface velocity data set for the 1990's over the Eastern Arctic from satellite SAR data can be downloaded from https://doi.pangaea.de/10.1594/PANGAEA.938381 (Strozzi et al., 2021).

1 Introduction

Glaciers and ice caps are retreating and thinning nearly everywhere in the world. Mass loss in recent decades was ascertained in various studies from a range of techniques and sensors, including glaciological observations (Zemp et al., 2019), satellite gravimetry observations (Wouters et al., 2019), differencing surface elevations from satellite and airborne observations (Hugonnet et al., 2021), and analysis of satellite interferometric altimetry (Tepes et al., 2021). In order to understand the mechanisms behind glacier mass loss and the discrepancies between the various studies, it is worthy to investigate the contributions of various components of mass loss. The calving flux of a glacier can be determined by multiplying its flow

https://doi.org/10.5194/essd-2022-44
Preprint. Discussion started: 17 February 2022


Open Access Earth System Science Data Discussions

velocity with its cross section at its grounding line (Paterson, 1994), so that for calving glaciers variations in flow velocities are directly related to the ice mass flux. Spatially and temporally consistent datasets of surface velocity are thus required to obtain the dynamic discharge component of mass loss from calving glaciers. An assessment of long-term trends and of seasonal variations would improve the related estimates. In addition, knowledge on ice surface velocity of glaciers and ice caps contributes to a better understanding of a wide range of glacial dynamics processes, for example flow modes and flow instabilities (e.g. surges), subglacial processes (e.g. erosion), supra- and intra-glacial mass transport, the development of glacier lakes and associated hazards, and improved estimates of ice thickness distribution. Satellite observations offer an appealing opportunity to reconstruct the evolution of glacier velocities back in time. Available ice surface velocity products such as GoLive (Global Land Ice Velocity Extraction from Landsat 8, Scambos et al., 2016), ITS-live (The Inter-mission Time Series of Land Ice Velocity and Elevation, Gardner et al., 2018) and the FAU-Glacier Portal (Global time series and temporal mosaics of glacier surface velocities derived from Sentinel-1 data of the Friedrich-Alexander-University Erlangen-Nürnberg, Friedl et al., 2021) have almost global coverage for the years since 2014 but not from before. In particular, data gaps exist for the Eastern Arctic from the 1990-2000 period due to the lack of good quality data from past Landsat missions.

The archives of past SAR sensors such as ERS-1/2 (1991-2010) and JERS-1 (1992-1998) are now freely and openly available. We exploit this opportunity to create datasets of ice surface velocity for the Eastern Arctic estimated for the 1990's using offset-tracking and SAR Interferometry (InSAR). The number of image pairs with suitable information available from these sensors, however, is limited in space and time, because these past sensors had irregular acquisition strategies and the orbital configurations put important constraints on obtaining good quality results. Hence, to retrieve spatially and temporally consistent datasets, regional velocity mosaics have to be created by compiling results from the best winter scene-pairs over several years. In this contribution, such nearly complete mosaics of ice surface velocities were computed for the 1990's for Novaya Zemlya, Franz-Josef-Land, Severnaya Zemlya and Svalbard.

We first describe the methods used to compute the ice surface velocity maps and give specific detailed description of the data products. In the following, we discuss long-term changes of winter ice surface velocities in the Eastern Arctic by comparing the 1990's mosaics to Sentinel-1 results of the winter 2020/2021. Where available, previously published velocity data derived from winter ALOS-1 PALSAR-1 data between 2008 and 2011 (Strozzi et al., 2017) are also included in our discussion about the spatial extent and magnitude of changes to highlight the temporal consistency of the trends or consider possible accelerating trends. Because glacier motion undergoes strong temporal variability, in particular on the seasonal time scale, one might ask in how far the mosaics, computed from SAR data over short time-intervals (typically 1 to 44 days) for several winter seasons in the 1990's, are representative of annual average results. To investigate this issue, we computed for a large number of glaciers dense time series of ice surface velocity from Sentinel-1 since 2015 and analysed short-term fluctuations in comparison to their annual means.

https://doi.org/10.5194/essd-2022-44
Preprint. Discussion started: 17 February 2022

2 Methods

2.1 Offset-tracking

Features that move on the surface of a glacier (e.g., crevasses, debris, radar speckle, etc.) can be tracked between two satellite images acquired at different times to measure ice surface displacement. The development of feature tracking algorithms based on intensity cross-correlation procedures is well established in glaciological studies and led to an automation of image processing with a related increase in efficiency and accuracy (Burgess et al., 2013; Paul et al., 2015; Dehecq et al., 2015; Nagler et al., 2015; Fahnestock et al., 2016; Strozzi et al., 2017). We employed the offset-tracking algorithm of the Gamma software (Strozzi et al., 2002; Werner et al., 2005) and considered the following data:

→ JERS-1 SAR data available from ESA (European Space Agency) as Single Look Complex (SLC) images (Level 1) and from JAXA (Japan Aerospace Exploration Agency) as RAW images (Level 0);

→ ERS-1/2 SAR data available from ESA as RAW images (Level 0);

→ ALOS-1 PALSAR-1 Fine Beam Single (FBS) data available from JAXA, ESA and ASF (Alaska Satellite Facility) as RAW images (Level 0);

→ IW (Interferometric Wide) Swath Sentinel-1 SAR data from Copernicus available as SLC (Level 1).

Image pairs were analysed for the same tracks and frames (Paul et al., 2015; Strozzi et al., 2017). Our main pre-processing steps included downloading of the data, optional focusing of RAW data to SLC images for Level 0 data, optional burst mosaic creation for Sentinel-1 data, and quality control. The main processing steps included geocoding of the reference image, co-registration of the slave image to the geometry of the master scene and offset-tracking via normalized intensity cross-correlation with the variable processing parameters listed in Table 1. In addition, multi-looked products such as differential interferograms and backscattering intensity and coherence images were computed. Digital Elevation Models (DEM) were used for the geocoding of the satellite SAR data, in order to derive three-dimensional ice surface displacement maps combining the slant-range and azimuth offsets by assuming that flow occurs parallel to the ice surface, and for differential interferometry. Over Svalbard, Novaya Zemlya and Franz-Josef-Land we used the TanDEM-X Intermediate DEM (IDEM) for that purpose, while for Severnaya Zemlya we used the digital elevation data derived from Soviet Union topographic maps of 1:100,000 and 1:200,000 scale as compiled by ViewfinderPanoramas (http://viewfinderpanoramas.org; last access: 6 September 2021). Both datasets are provided in 3 arcsec resolution and geographic coordinates (Strozzi et al., 2017). The main post-processing steps included filtering of noise, mitigation of ionospheric azimuth streaks based on high-pass filtering along the range direction (Wegmüller et al., 2006), geocoding, computation of statistical measures over ice-free regions, and final velocity product creation.

https://doi.org/10.5194/essd-2022-44
Preprint. Discussion started: 17 February 2022

The archive of JERS-1 data at ESA was systematically mined and all image pairs in series from the same track and frame were analysed. Only results obtained for 44-day winter image pairs were further considered, because in summer and over longer time periods the ice surface velocity maps contained much noise and reduced spatial coverage. Where no 44-day winter JERS-1 image pairs were found in the ESA archive, the JERS-1 data archive at JAXA was searched to complement the results. Further data gaps existed for the far east of Franz-Josef-Land, entire Severnaya Zemlya and the central part of Svalbard. In these regions we tracked ERS-1 data with time intervals of 9 to 18 days.

Table 1. Processing parameters for different sensors.

Sensor	Slant-Range Pixel Spacing	Incidence Angle	Azimuth Pixel Spacing	InSAR Multi-Looking	Tracking Template Size	Tracking Step
JERS-1	8.8 m	39 degrees	4.5 m	4 x 12 (55 m x 54 m)	64 x 256 (887 m x 1153 m)	10 x 30 (139 m x135 m)
ERS-1	7.9 m	23 degrees	3.9 m	2 x 10 (40 m x 40 m)	128 x 512 (2557 m x 2018 m)	8 x 32 (160 m x 126 m)
ALOS-1 PALSAR-1	4.7 m	39 degrees	3.1 m	4 x 8 (30 m x 25 m)	64 x 192 (478 m x 595 m)	12 x 36 (90 m x 112 m)
Sentinel-1	2.3 m	39 degrees	13.9 m	20 x 4 (74 m x 56 m)	512 x 128 (1892 m x1777 m)	40 x 10 (148 m x139 m)

2.2 SAR interferometry

The use of differential SAR interferometry to map surface displacements at centimetre-resolution is well established in research and operational projects (Luckman et al, 2002; Dowdeswell et al., 2008; McMillan et al., 2014). The interferometric phase is sensitive to both surface topography and coherent displacement along the look vector occurring between the two acquisitions of the interferometric image pair. The differential use of a high-resolution DEM (2-pass InSAR) or of two SAR image pairs acquired within short time periods (3/4-pass InSAR) allow the removal of the topographic phase from the interferogram to derive a displacement map. In the case of 2-pass InSAR, the acquisition date of the DEM has to match that of the SAR dataset close enough to ensure that no major topographic signal is left on the differential interferograms. In the case of 3/4-pass InSAR, displacement within the two image pairs is assumed constant. In addition, short perpendicular baselines of the SAR image pairs are preferred, in order to minimize the effect of the residual topographic phase so that phase signals can be interpreted as ice surface displacement in the satellite line-of-sight direction, with possible atmospheric disturbances.

ERS-1/2 InSAR results from previous studies (Dowdeswell et al., 2008; Nuth et al., 2019) were considered to improve the quality and completeness of the results over Nordaustlandet, south Spitsbergen and north-west Spitsbergen (Svalbard). The ERS-1/2 InSAR ice velocity map of Nordaustlandet combines interferometric phases from 1-day ERS-1/2 image pairs and is produced for the winter 1995/1996 at 100 m resolution. Method and uncertainties are described in Dowdeswell et al. (2008). In most cases errors are assumed to be smaller than 7 m/a, while for unfavourable combinations of image pairs this value is slightly larger. The ERS-1/2 InSAR ice velocity map of south Spitsbergen is produced from winter 1996 and 1997 data at 20

https://doi.org/10.5194/essd-2022-44
Preprint. Discussion started: 17 February 2022

m resolution. Method and uncertainties are described in Nuth et al. (2019). The accuracy was measured by extracting displacements across a point grid of 1000 m spacing excluding points which were not on stable terrain (glaciers, fjords, etc.). Nuth et al. (2019) found a median value of 2.3 m/a and a standard deviation of 2.6 m/a. The same processing and accuracy assessment procedure was also applied to 1-day ERS-1/2 image pairs of winter 1995/1996 over north-west Spitsbergen . In this case, a median value of 4.0 m/a and a standard deviation of 3.7 m/a were found.

3 Data

Two sets of data containing ice surface velocities over the Eastern Arctic can be downloaded from https://doi.pangaea.de/10.1594/PANGAEA.938381. The first set of data contains the velocities derived from offset-tracking of all image tracks from this study as original research data in vector format with metadata information. Nine collections of data wrapped up in single files for easy storage (tar packaging followed by a gzip compression) are available: the JERS-1 (1992-1998) results over Novaya Zemlya, Franz-Josef-Land, and Svalbard, the ERS-1 (1991-1992) results over Franz-Josef-Land, Severnaya Zemlya and Svalbard and the ALOS-1 PALSAR-1 (2006-2011) results over Novaya Zemlya, Franz-Josef-Land, and Svalbard. A comma-separated values file (.csv) provides the northing and easting coordinates of measurement points, the elevation from the above-mentioned DEMs, the displacement in metres in the x, y and z directions and the cross-correlation coefficient for each measurement. A metadata file in extensible markup language format (.xml) provides information about the SAR images (<inputSatelliteData1> and <inputSatelliteData2>), the processing parameters (<processingParameters>) and quality aspects of the data such as the percent of valid information over ice (<QA-IV-2>) and statistical measures over ice-free regions (<QA-IV-3>). In addition, the original research data packages include for each image pair GeoTIFF files of the three-dimensional ice surface displacement maps (.tif in single-precision floating-point format and .300.tif as exemplary display of the colour-coded displacement map with saturation at 300 m/a), the two intensity images (.pwr1.tif and .pwr2.tif), the differential interferogram (.tflt.tif), the phase coherence image (.cc.tif), an RGB colour composite of the coherence, intensity and intensity difference between both images (.rgb.tif), and the layover and shadow map (.ls_map.tif. In all cases data are provided the Universal Transverse Mercator (UTM) projection (zones 33N for Svalbard, 40N for Novaya Zemlya and Franz-Josef Land, and 47N for Severnaya Zemlya) with a spatial resolution of 100 m.

The second set of data contains velocity mosaics of the best JERS-1 results over Novaya Zemlya, Franz-Josef-Land, and Svalbard, the best ERS-1 results over Franz-Josef-Land, Severnaya Zemlya and Svalbard and the best ALOS-1 PALSAR-1 results over Novaya Zemlya, Franz-Josef-Land, and Svalbard in GeoTIFF format. In addition, we provide in the same format also the winter ERS-1/2 InSAR ice velocity map, used to improve the quality of the results over Svalbard, and Sentinel-1 mosaics computed from winter 2020/2021 data, considered in the following section to study the long-term variability of winter ice surface velocity over the Eastern Arctic. Appendix A provides the lists of the satellite data considered over the four study regions along with some technical information and Figure 1 shows the SAR footprints.

https://doi.org/10.5194/essd-2022-44
Preprint. Discussion started: 17 February 2022

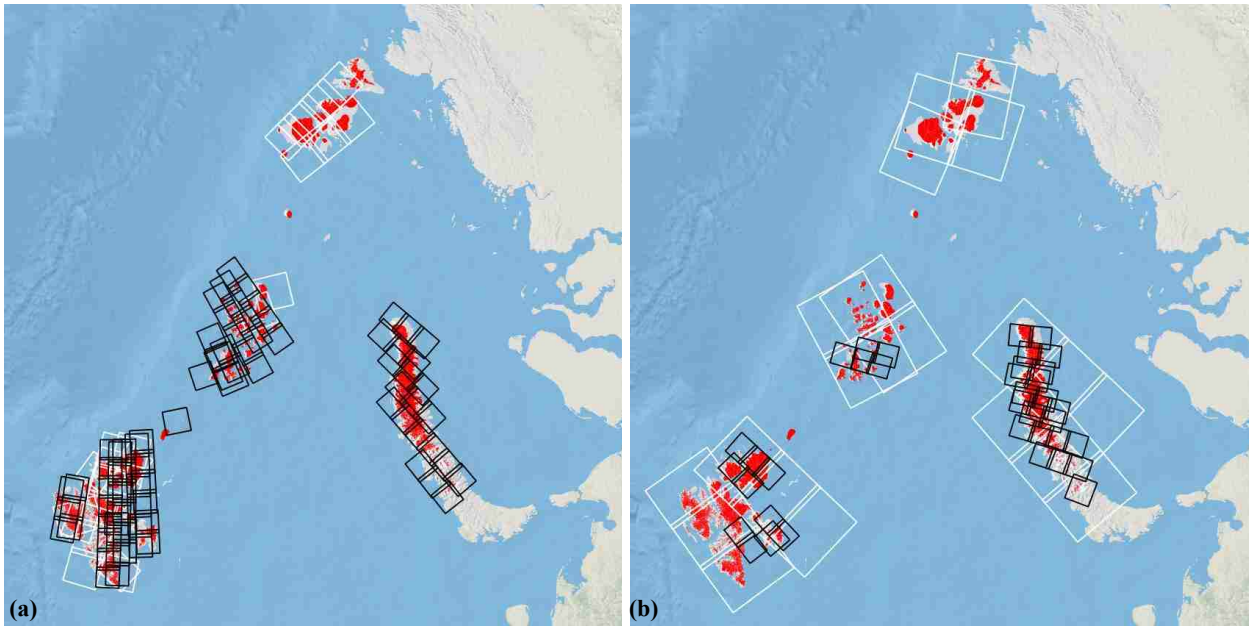

Figure 1: a) JERS-1 (black) and ERS-1 (white) SAR footprints. b) ALOS-1 (black) and Sentinel-1 (white) SAR footprints.

4 Results

4.1 Flow velocities for distinct periods

Mosaics of ice velocity maps of the 1990's for Novaya Zemlya, Franz-Josef-Land, Severnaya Zemlya and Svalbard are presented in Figures 2a, 4a, 5a, and 6a, respectively. In the Russian High Arctic, priority in the winter ice velocity mosaics was given to JERS-1 offset-tracking over ERS-1 offset-tracking. Glaciers were masked out from land and sea using glacier outlines from satellite imagery acquired between 2000 and 2010 during summer (Moholdt et al., 2012), after manual adjustment using the SAR backscattering intensity images of the front position of the glaciers that significantly retreated or advanced from the 1990's to the 2000's. In addition, for Severnaya Zemlya we included ice flow over the Matusevich Ice Shelf that collapsed in 2012 (Willis et al., 2015). Over Svalbard, priority in the winter ice velocity mosaic was given to ERS-1/2 InSAR over JERS-1 offset-tracking, with ERS-1 offset-tracking considered to fill minor data gaps over north-east Spitsbergen. Over this region we considered the glacier outlines from summer satellite imagery spanning the period 2000-2010 (Nuth et al., 2013) after correction from the SAR backscattering intensity images for the front position of the major retreating or advancing glaciers.

https://doi.org/10.5194/essd-2022-44
Preprint. Discussion started: 17 February 2022

Sentinel-1 mosaics computed from winter 2020/2021 data that showed the best spatial coverage are considered to study the long-term variability of winter ice surface velocity. The four Sentinel-1 velocity maps for Novaya Zemlya, Franz-Josef-Land, Severnaya Zemlya and Svalbard are shown in Figures 2c, 4b, 5b and 6b, respectively. Glaciers were masked out from land and sea using satellite imagery acquired between 2013 and 2016 over Novaya Zemlya (Rastner et al., 2017), in 2016 for Franz-Josef-Land (unpublished), between 2000 and 2010 over Severnaya Zemlya (Moholdt et al., 2012) with additional manual adjustment of the surge over the Vavilov Ice Cap, and between 2016 and 2018 for Svalbard (unpublished). Difference maps between the 1990's and 2020/2021 velocity data were computed for all study regions only where the 2020/2021 Sentinel-1 ice velocities are larger than 50 m/a. Figures 3c, 4c, 5c and 6c show the difference maps for Novaya Zemlya, Franz-Josef-Land, Severnaya Zemlya and Svalbard, respectively. Only areas within the newest glacier inventories for Novaya Zemlya (Rastner et al., 2017), Franz-Josef-Land (unpublished) and Svalbard (unpublished) and the Randolph Glacier Inventory (RGI) 6.0 for Severnaya Zemlya (Moholdt et al., 2012) are included.

Where available, we include in our discussion previously published velocity results from ALOS-1 PALSAR-1 (Strozzi et al., 2017) in order to highlight the temporal consistency of the changes or point to possible trends and differences. In particular, we consider a nearly complete mosaic computed for Novaya Zemlya from winter ALOS-1 PALSAR-1 data acquired between 2008 and 2010. This mosaic is shown in Figure 2b with glaciers masked out from land and sea using glacier outlines from satellite imagery acquired between 2000 and 2010 during summer (Moholdt et al., 2012). The difference maps between the 1990's and 2000's velocity maps and between the 2000's and 2020/2021 velocity maps for Novaya Zemlya are shown in Figures 3a and 3b, respectively. For the other regions, only very limited scattered results are available from ALOS-1 PALSAR-1 between 2008 and 2011, which are discussed in Section 4.2.

4.2 Long-term variability of ice surface velocity

4.2.1 Novaya Zemlya

Over the western coast of Novaya Zemlya along the Barents Sea coast, where marine-terminating glaciers have the highest frontal velocities of the archipelago (Figure 2), we observe an increase in frontal velocities from 1998 to 2021 for all the 18 major outlet glaciers with Sentinel-1 winter 2021 velocities larger than 100 m/a (Figure 3c). In most of the cases, the increase of frontal velocities exceeds 100 m/a and is spread over a large frontal part of the outlet glaciers. In only a few cases frontal velocities in 1998 and 2021 were similar, but the retreat of the glacier front since 1998 and a larger area with fast velocity in 2021 resulted in a strong signal in Figure 3c. Over the eastern coast of Novaya Zemlya we observe an increase of frontal velocity of more than 100 m/a from 1998 to 2021 over 8 of the >15 major outlet glaciers. The spatial extent of the frontal velocity increase is more limited across the eastern coast than the western coast. For all the 26 outlet glaciers with significant velocity changes, the front retreated from 1998 to 2021. The analysis of the ALOS-1 SAR data of 2008-2010 shows that the general increase of frontal velocities along with a retreat of frontal positions over Novaya Zemlya is

https://doi.org/10.5194/essd-2022-44
Preprint. Discussion started: 17 February 2022

particularly evident in recent years (Figure 3b), indicating an enhanced trend of velocity increase in more recent periods. The general pattern of ice velocity changes between 1998 and 2008-2010 is more contrasted (Figure 3a), with at least five glaciers along the western coast of Novaya Zemlya showing a decrease in frontal velocities. Apart from Severny Island 1 Glacier, we did not detect any sign of destabilisation for the glaciers on Novaya Zemlya. In this region the inter-annual changes of winter ice surface velocity between 1998 and 2021 exceed seasonal variability (Figure 11) and can be considered a significant representation of the long-term variability of ice surface velocity over this region.

4.2.2 Franz-Josef-Land

Over Franz-Josef-Land, the general pattern of the differences between winter ice surface velocities from the 1990's to 2020/2021 is dominated by glaciers with an increase in frontal velocities in recent years (Figure 4c). We observe, however, also at least three glaciers with a clear (i.e., <-50 m/a) decrease of frontal speeds. Glacier fronts generally retreated from the 1990's to 2020/2021, with two exceptions. Simony Glacier on McClintock Island advanced by about 800 m from 1998 to 2021 and probably underwent a frontal destabilisation in the early 2010's (Strozzi et. al. 2017). The most west-oriented glacier of the Tyndal Ice Cap on Hall Island advanced by nearly 500 m from 2017 to 2019 to reach in 2021 approximately the same position as in 1998. ALOS-1 PALSAR-1 winter image pairs were acquired only over the western part of Franz-Josef-Land in 2010-2011 (Figure 1b). Already between 1996-1998 and 2010-2011 (Figure 7a) we observe a general increase of ice velocity, which continued for many (but not all) glaciers between 2010-2011 and 2021 (Figure 7b) so that the general patterns of changes from the 1990's to 2021 are dominated by glaciers with an increase in frontal velocities (Figure 7c). Over Franz-Josef-Land, we did not detect any clear sign of destabilisation and the inter-annual changes of winter ice surface velocity, which exceed seasonal variability, can be considered representative of the long-term variability of ice surface velocity.

4.2.3 Severnaya Zemlya

Changes in the ice surface velocity observed between the 1990's and 2020/2021 over Severnaya Zemlya (Figure 5c) are more prominent than over Novaya Zemlya (Figure 3c) and Franz-Josef-Land (Figure 4c). While there are larger errors from the ERS-1 data (Figure 5a) available for this region than for JERS-1 data for Novaya Zemlya and Franz-Josef-Land (Figures 2a and 4a), these results have better spatial coverage than those available from previous studies with winter ERS-1/2 InSAR data (Dowdeswell et al., 2002) and summer ALOS-1 PALSAR-1 data (Strozzi et al., 2017). Over the Academy of Sciences Ice Cap, we observe a widespread increase of ice surface velocities from 1991 to 2020/2021 of more than 100 m/a for five large and two small glaciers. For two glaciers over this ice cap, the maximum speeds at the front were actually higher in 1991 than in 2020/2021. This is not reflected in Figure 5c, however, due to the retreat of the glaciers. Over the Vavilov Ice Cap, we observe a widespread increase of ice surface velocities from 1991 to 2020/2021, where a surge possibly followed by the transition to an ice stream is occurring since 2015 (Glazovsky et al., 2015; Willis et al., 2018; Zheng et al., 2019). It is worth mentioning that the ERS-1 records indicate stagnant ice over large parts of the Vavilov Ice Cap in 1991. Other smaller

https://doi.org/10.5194/essd-2022-44
Preprint. Discussion started: 17 February 2022

regions with an increase of speed are recorded over the Rusanov Ice Cap (four glaciers) and Karpinsky Ice Cap (two). To the north of the Karpinsky Ice Cap, one glacier had significantly larger velocities in 1991 compared to 2020/2021, which is visible by blue colours in Figure 5c. Prior to the collapse of the Matusevich Ice Shelf in 2012 (Willis et al., 2015), this glacier largely extended across the sea between the Karpinsky and Rusanov Ice Caps. Over Severnaya Zemlya, we again observe a general retreat of frontal positions from 1991 to 2020/2021. The only two exceptions are the surging outlet glacier of the Vavilov Ice Cap and one glacier flowing towards south over the Academy of Sciences Ice Cap with stagnant ice in 1991 (Figure 5a) and a high velocity in 2020/2021 (Figure 5b). Over Severnaya Zemlya there were unfortunately no suitable winter ALOS-1 PALSAR-1 acquisitions to compute ice surface velocities over 46 days at the end of the 2000's. Over Severnaya Zemlya, we detected two glaciers with clear signs of destabilisation. Also for these, however, the inter-annual changes of winter ice surface velocity, which exceed seasonal variability, again represent the long-term variability of ice surface velocity rather well.

4.2.4 Svalbard

The difference map between ice surface velocities in the 1990's and 2021 for areas with Sentinel-1 velocities larger than 50 m/a over Svalbard (Figure 6c) shows a large increase of velocities for many glaciers. Along with glaciers having significantly higher frontal velocities (e.g., Monacobreen, Kronebreen and Osbornbreen on Spitsbergen and Schweigaardbreen, Leighbreen, and Basin 7 on Austfonna), there are also many prominent surges, e.g., Basin 3 (Austfonna), Stonebreen (Edgeyoa), Negribreen and Sonklarbreen (Spitsbergen) and a few other smaller ones. Over south Spitsbergen we observe the only glacier with significantly higher velocities in the 1990's, Mendelejevbreen, which surged apprixmately in 2000 (Blaszczyk et al., 2009). Other large glaciers that were surging during the 1990's, such as Monacobreen in 1994 (Luckman et al., 2002) and Fridtjovbreen in 1996 (Murray et al., 2003), are not captured in our mosaic shown in Figure 6a, because the data were from either after (1998 in the case of Monacobreen) or before (1992 in the case of Fridtjovbreen) the peak of the surges. Additionally, also for other large glaciers that surged between the 1990's and 2021, such as Tunabreen in 2004 (Flink et al., 2015), Nathorsbreen in 2009 (Sund et al., 2014; Nuth et al., 2019), Basin 2 in 2015 (Schellenberger et al., 2017) and Strongbreen in 2016 (Benn et al., 2019), there are no signals visible in Figure 6c. The signals of the surges of Strongbreen and Basin 2, however, are captured well in Sentinel-1 images of the years prior to 2021, when flow over these two glaciers became stagnant after the surge (Friedl et al., 2021). The overview of frontal position changes between the 1990's and 2021 over Svalbard has more contrasts than over the other three study regions. Again, we observe a general retreat of frontal positions, but there are also strong advances for recently surging glaciers (e.g., Negribreen, Sonklarbreen, Nathorstbreen, Strongbreen, Basin 3 and Basin 2). Other glaciers such as Basin 7 and Stonebreen have nearly the same position in 2021 as in the 1990's, with a retreat from 1990's to 2015 compensated by a recent advance. Tunabreen is also nearly at the same frontal position in 2021 as in the 1990's, by reason of a surge in 2004 and a further surge-like advance in 2017/2018. The front of Fridtjovbreen, which surged in 1996, is still more advanced in 2021 than in 1991. ALOS-1 PALSAR-1 winter image pairs were acquired only over the eastern part of Svalbard in 2008-2011 (Figure 1b). Already

https://doi.org/10.5194/essd-2022-44
Preprint. Discussion started: 17 February 2022

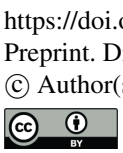

between the 1990's and 2008 (Figure 8a), we observe a general increase of ice velocity over Nordaustlandet, which continued for nearly all glaciers until 2021 (Figure 8b). A slight decrease of ice velocity between 2008 and 2021, however, is visible over Duvebreen and Franklinbreen, which both underwent an active surge initiated in winter 1998/99 (Pohjola et al., 2011). A strong increase of ice velocity between 2011 and 2021 is observed in Figure 8b also over Stonebreen (Edgeyoa), while the surges of Negribreen and Sonklarbreen are not visible in Figure 8b, because they are not covered by ALOS-1 PALSAR-1. Due to the colour saturation at 100 m/a, the very strong increase of velocities over Basin 3 is actually underlined in Figures 8b and 8c. The long-term variability of ice surface velocity from a mosaic computed over short-time intervals from several years is much less representative of yearly averages over Svalbard than over the three other study regions, even without taking into account that over this region a large number of glaciers (more than ten according to Leclercq et al. (2021)) underwent surging events in recent years.

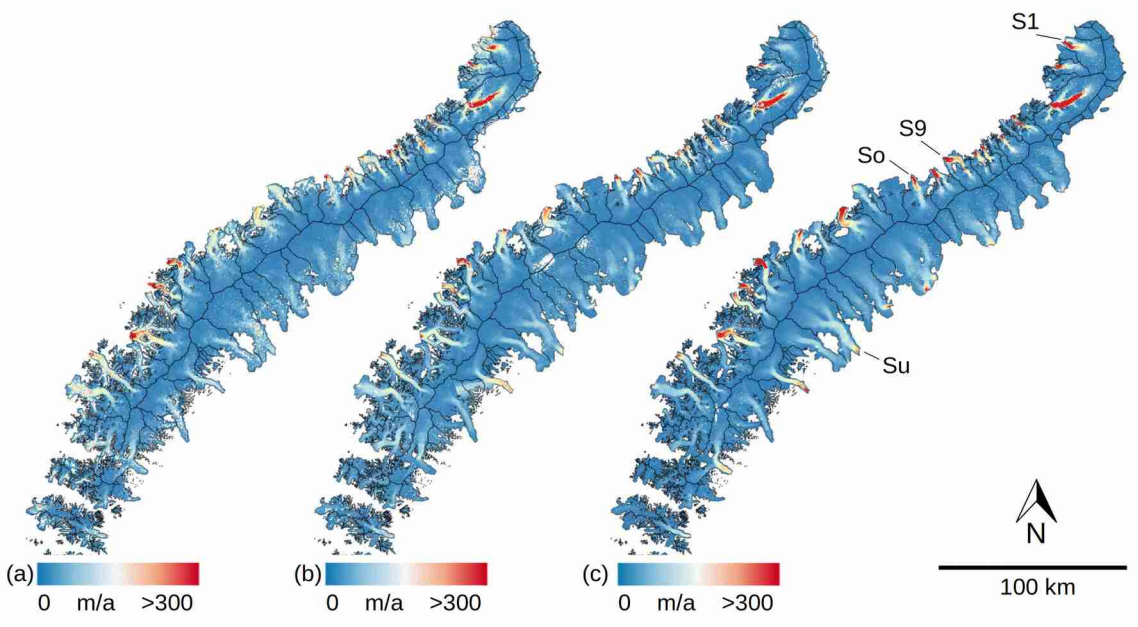

Figure 2: Ice velocity maps for Novaya Zemlya: (a) JERS-1 1998.01.21-1998.03.25, (b) ALOS-1 2008.12.11-2010.04.29, (c) Sentinel-1 2021.02.04-2021.02.25. Glacier outlines from Rastner et al. (2017). Letters refer to glaciers mentioned in the text (Su: Shury; So: Shokalskiy; S1: Severny Island 1; S9: Severny Island 9).

https://doi.org/10.5194/essd-2022-44
Preprint. Discussion started: 17 February 2022

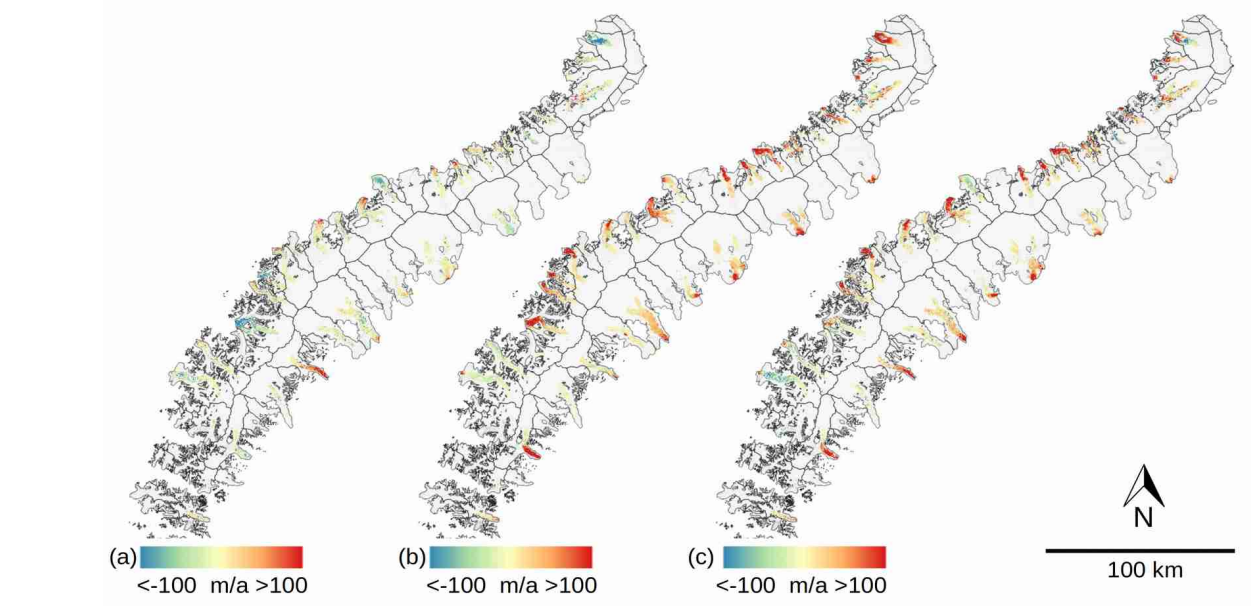

Figure 3: Difference maps for areas with Sentinel-1 2021 velocity larger than 50 m/a for Novaya Zemlya: (a) ALOS-1 - JERS-1, (b) Sentinel-1 - ALOS-1, (c) Sentinel-1 - JERS-1. Glacier outlines from Rastner et al. (2017). JERS-1 data were acquired in 1998, ALOS-1 PALSAR-1 in 2008-2011 and Sentinel-1 in 2021.

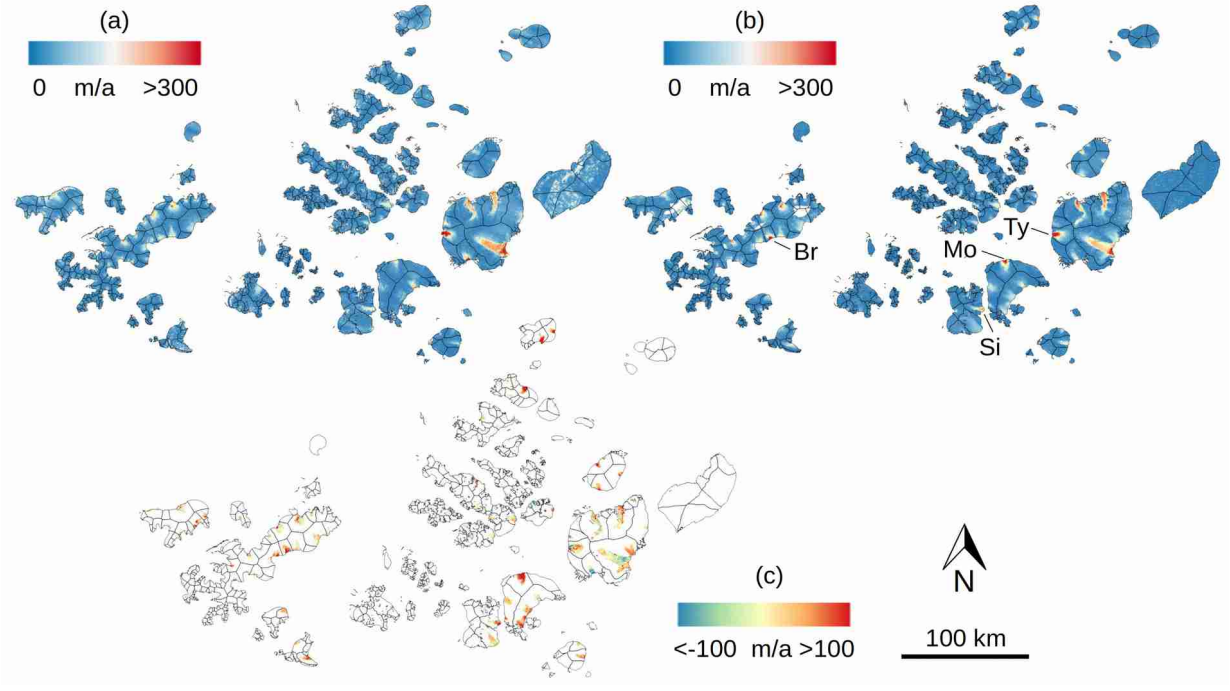

Figure 4: Ice velocity maps for Franz-Josef-Land: (a) JERS1 1996.04.04-1998.05.29 & ERS1 1991.10.12-1991.11.17, (b) Sentinel-1 2021.01.10-2021.02.12. (c) Difference map for areas with Sentinel-1 velocity >50 m/a. Glacier outlines from 2016 (unpublished). Letters refer to glaciers (Si: Simony) and ice caps (Ty: Tyndal; Mo: Moscow; Br: Brousilov) mentioned in the text.

https://doi.org/10.5194/essd-2022-44
Preprint. Discussion started: 17 February 2022

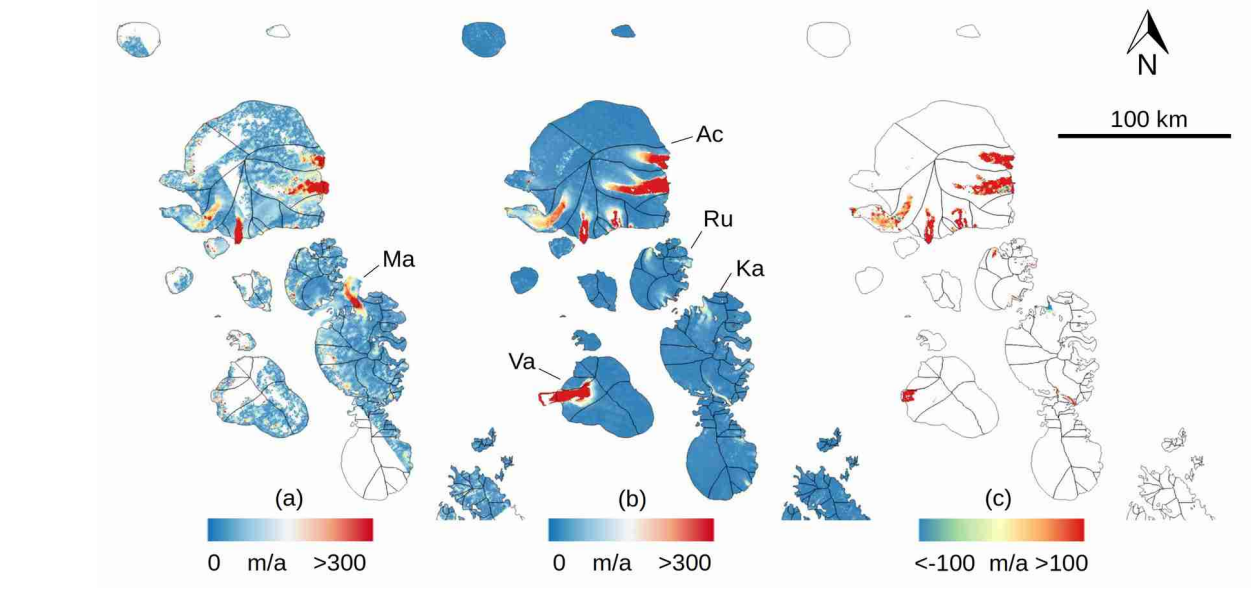

295

Figure 5: Ice velocity maps for Severnaya Zemlya: (a) ERS1 1991.10.18-1992.03.02, (b) Sentinel-1 2020.12.15-2021.02.25. (c) Difference map for areas with Sentinel-1 velocity >50 m/a. Glacier outlines from RGI 6.0 (Moholdt et al., 2012). Letters refer to the Matusevich Ice Shelf (Ma) and ice caps mentioned in the text (Ac: Academy of Sciences; Va: Vavilov; Ka: Karpinsky; Ru: Rusanov).

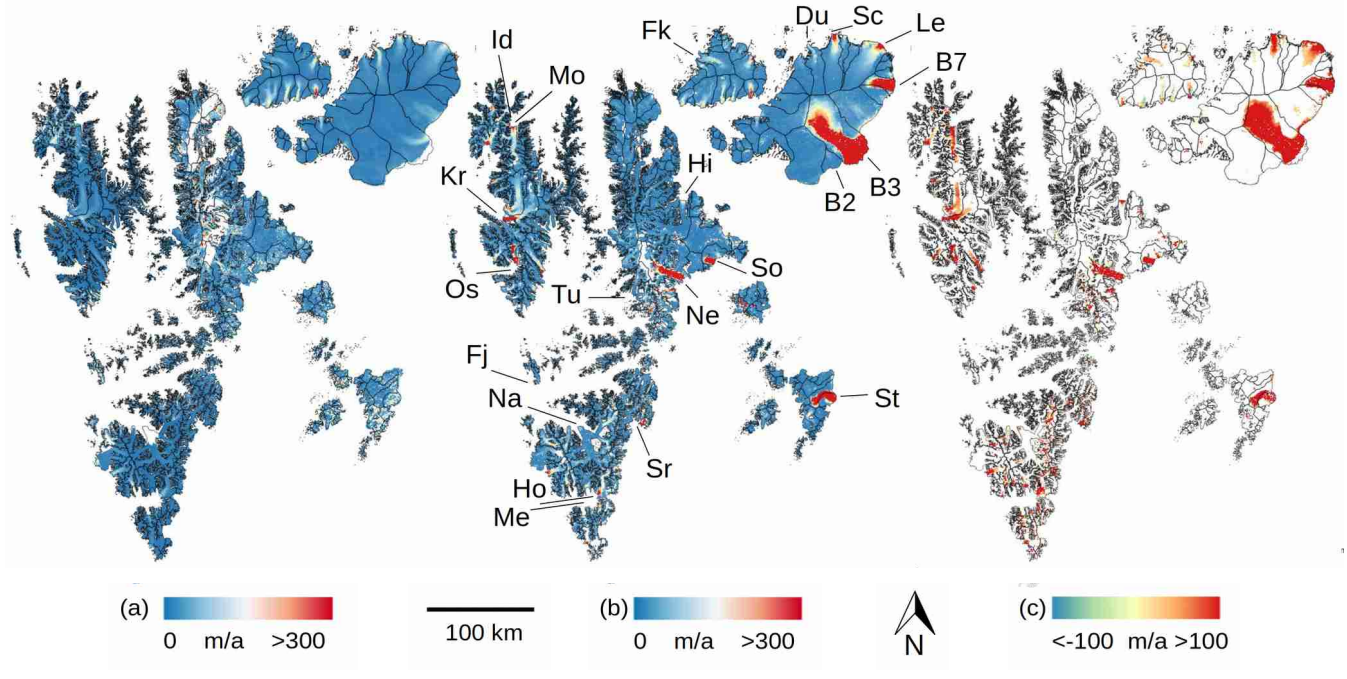

300

Figure 6: Ice velocity maps for Svalbard: (a) ERS-1/2 1995.12.10-1995.01.29 & JERS1 1994.02.05-1998.03.26 & ERS-1 1992.01.03-1992.01.15 and (b) Sentinel-1 2021.01.26-2021.02.12. (c) Difference map for areas with Sentinel-1 velocity >50 m/a. Glacier outlines between 2016 and 2018 (unpublished). Letters refer to glaciers mentioned in the text (Mo: Monacobreen; Id: Idabreen; Kr:
305 **Kronebreen; Os: Osbornbreen; Hi: Hinlopenbreen; Tu: Tunabreen; Ne: Negribreen; So: Sonklarbreen; Fj: Fridtjovbreen; Na:**

https://doi.org/10.5194/essd-2022-44
Preprint. Discussion started: 17 February 2022

Open Access Earth System Science Data Discussions

Nathorsbreen; Sr: Strongbreen; Ho: Hornbreen; Me: Mendelejevbreen; Fk: Franklinbreen; Du: Duvebreen; Sc: Schweigaardbreen; Le: Leighbreen; B2: Basin 2; B3: Basin 3; B7: Basin 7; St: Stonebreen).

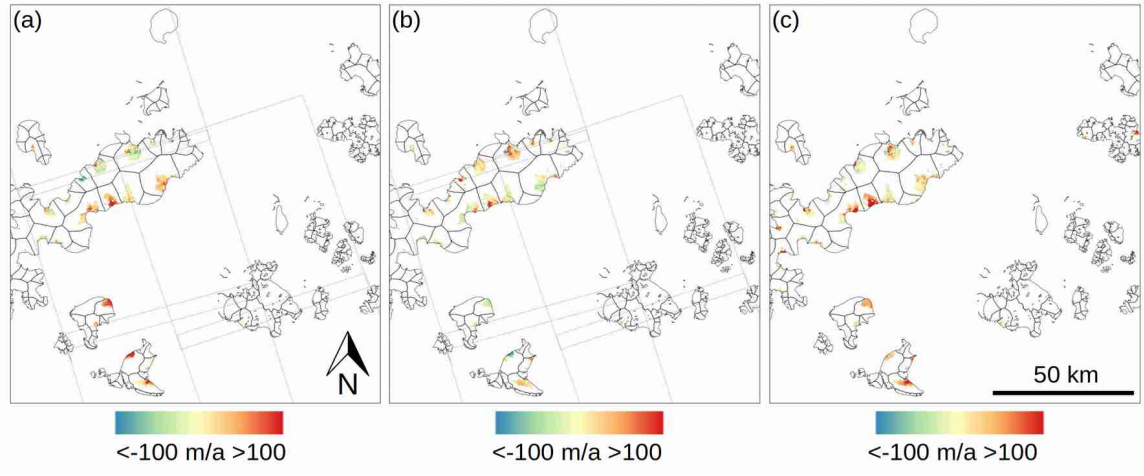

Figure 7: Difference maps for areas with Sentinel-1 2021 velocity larger than 50 m/a for western Franz-Josef-Land: (a) ALOS-1 - JERS-1, (b) Sentinel-1 - ALOS-1, (c) Sentinel-1 - JERS-1. Glacier outlines from 2016 (unpublished). ALOS-1 SAR footprints are shown in (a) and (b). JERS-1 data were acquired in 1991-1998, ALOS-1 PALSAR-1 in 2010-2011 and Sentinel-1 in 2021.

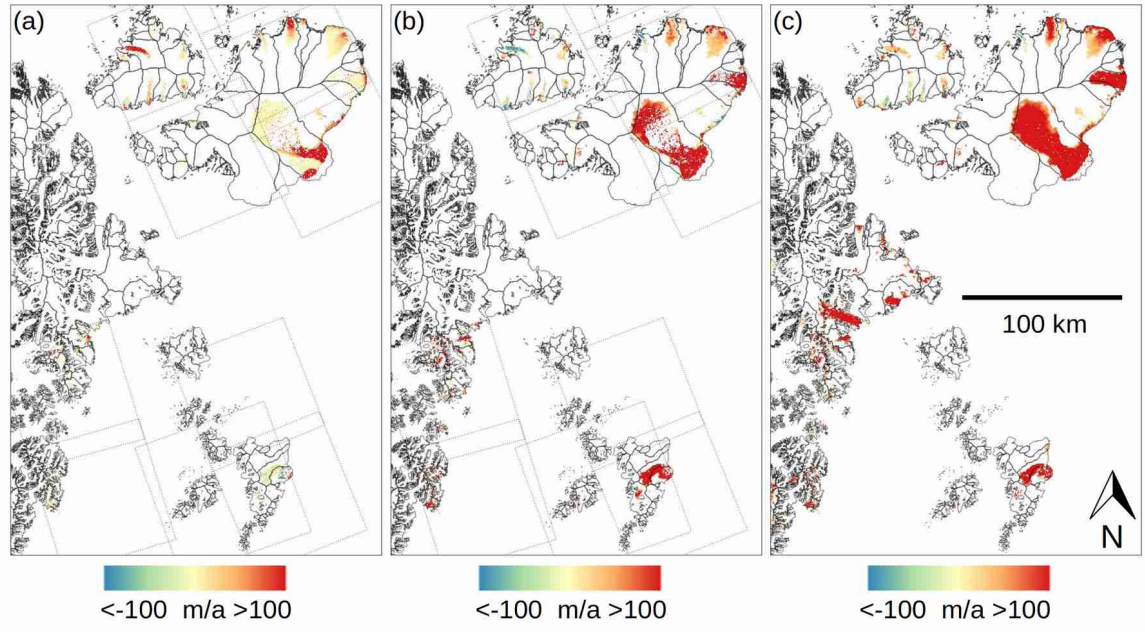

Figure 8: Difference maps for areas with Sentinel-1 2021 velocity larger than 50 m/a for eastern Svalbard: (a) ALOS-1 - JERS-1, (b) Sentinel-1 - ALOS-1, (c) Sentinel-1 - JERS-1. Glacier outlines between 2016 and 2018 (unpublished). ALOS-1 SAR footprints are shown in (a) and (b). JERS-1 data were acquired in 1992-1998, ALOS-1 PALSAR-1 in 2008-2011 and Sentinel-1 in 2021.

https://doi.org/10.5194/essd-2022-44
Preprint. Discussion started: 17 February 2022

5 Discussion

5.1 Error sources: product quality and seasonal variability of ice surface velocity

Uncertainties in winter ice surface velocity estimations originate from errors in tracking offsets between image pairs as well as unknown representativeness of winter velocity mosaics with regard to the annual average velocities. Paul et al. (2017) extensively discussed the factors influencing the product quality and described various measures to determine precision and accuracy. External factors influencing product quality include glacier surface conditions, structure and terrain complexity and ionospheric scintillations. Internal factors influencing product quality include the choice of the matching window size and oversampling factor and the post-processing to filter the noise of the resulting estimates. Validation of glacier displacements measured from spaceborne sensors compared to ground-based data is inherently difficult, because it requires temporally consistent in-situ and satellite observations of similar spatial scale and displacement direction. Therefore, uncertainties in velocity-based products are frequently characterized based on internal measures. Here, we do not reiterate the numerous internal measures that exist to validate the data, but make reference to previous work. In particular, according to previous studies, our SAR-derived velocities have uncertainties of ±20 m/a for JERS-1 (Strozzi et al., 2008), ±40 m/a for ERS-1 (Dowdeswell et al., 2008), ±10 m/a for ALOS-1 PALSAR-1 (Paul et al., 2015) and ±20 m/a for Sentinel-1 (Strozzi et al., 2017). More specific quality aspects, such as a comment from an experienced operator based on visual inspection of the resulting displacements (<QA-IV-1>, if applicable), the percent of valid information over ice (<QA-IV-2>) and statistical measures over ice-free regions (<QA-IV-3>), are given in the metadata information of each dataset (.xml). These quality aspects are listed in Appendix A for the data considered in the velocitiy mosaics. The characterisation of the matching quality of individual ice velocity estimates is also given by the cross-correlation coefficient given in the comma-separated values file (.csv).

In order to infer in how far the mosaics computed from SAR data over short time-intervals (typically 1 to 44 days) for several winter seasons in the 1990's are representative of annual average results, we analyse short-term variability in glacier flow from Sentinel-1 data regularly available since 2015 with 12-day repetition rate. While ice velocity maps derived for winter with Sentinel-1 have an excellent coverage of valid information over both the interior of the ice caps and the outlet glaciers, summer results are often limited to the crevassed outlet glaciers, because surface melt strongly alters the appearance of other surface features in SAR intensity images. For a large number of glaciers showing Sentinel-1 winter velocities larger than 100 m/a, we selected one representative point close to each glacier front and extracted time series of velocities computed every 12 days. Examples of time series for glaciers over Novaya Zemlya, Franz-Josef-Land, Severnaya Zemlya and Svalbard with distinctly different patterns are shown in Figures 9 to 12. In addition, we computed an annual average ice surface velocity and compared it to winter (October-May) and summer (June-September) averages. A linear trend was not subtracted from this comparison, although there are some signs of changes. Figure 13 graphically summarises the percentage

https://doi.org/10.5194/essd-2022-44
Preprint. Discussion started: 17 February 2022

differences between winter and summer velocities compared to annual averages for the selected glaciers over the four study regions. Appendix B lists the statistics for all the glaciers analysed in our study. The time series of ice surface velocities for the 26 glaciers analysed in our study on Novaya Zemlya, the 27 glaciers analysed over Franz-Josef-Land, the 17 glaciers analysed over Severnaya Zemlya, and the 30 glaciers analysed over Svalbard, all with Sentinel-1 velocities larger than 100 m/a, are shown in Appendix C.

5.1.1 Novaya Zemlya

The time series of every glacier display characteristic patterns, with possible year-to-year (e.g., accelerations, decelerations, pulses, destabilisations or surges) and seasonal (e.g., summer speed-up events, generally higher summer or winter velocities) changes. Shury Glacier on Novaya Zemlya (Figure 9a) is, for instance, characterised by short-term, strong summer accelerations. Shokalskiy Glacier (Figure 9b) generally flows faster in winter than in summer, but also has summer accelerations. Severny Island 1 Glacier (Figure 9c) shows an increase in velocity from 2017 to 2021 with higher summer values. The front of this glacier also advanced by more than 300 m from 2015 to 2021. For the 26 glaciers on Novaya Zemlya with Sentinel-1 velocities larger than 100 m/a, the velocities in the winter period differed between -12% and +4% (average -3%) from the average annual velocities. For the summer period, the related differences were between +33% and -12% (average +8%). Summer differences are larger than those in winter, because the summer speed-ups are short, intensive events and the summer period is shorter.

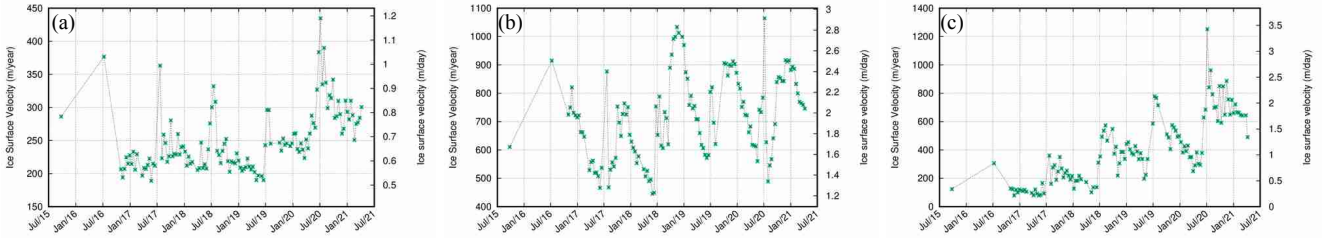

Figure 9: Novaya Zemlya: time series of Sentinel-1 velocity for (a) Shury Glacier (mean 250 m/a, mean summer 280 m/a (+11.8%), mean winter 238 m/a (-4.8%)), (b) Shokalskiy Glacier (mean 719 m/a, mean summer 671 m/a (-6.8%), mean winter 737 m/a (+2.5%)) and (c) Severny Island 1 (mean 396 m/a, mean summer 507 m/a (+27.9%), mean winter 356 m/a (-10.2%)).

5.1.2 Franz-Josef-Land

Over Franz-Josef-Land the Sentinel-1 acquisitions stopped in 2018-2019 and the time series of Figure 10 are incomplete and more difficult to interpret. Simony Glacier on McClintock Island (Figure 10a), which advanced by about 800 m from 1998 to 2021 and underwent a frontal destabilisation in the early 2010's (Strozzi et al., 2017), shows generally decreasing velocities from 2015 to 2021 with strong summer speed-up events. The west-oriented glacier of the Tyndal Ice Cap on Hall Island (Figure 10b), which advanced by nearly 500 m from 2017 to 2019, had similar velocities in 2017/2018 and 2020 and lower

https://doi.org/10.5194/essd-2022-44
Preprint. Discussion started: 17 February 2022

Open Access Earth System Science Data Discussions

ones in 2021, but the most interesting period in 2018-2019 is missing. A glacier on Moscow Ice Cap shows strong summer speed-up events followed by slowly decreasing values (Figure 10c). For the 27 glaciers analysed over Franz-Josef-Land with Sentinel-1 velocities larger than 100 m/a, the velocities in the winter period differed between -11% and +3% (average -3%) from the average annual velocities. In the warm period, they differed between +43% and -11% (average +12%).

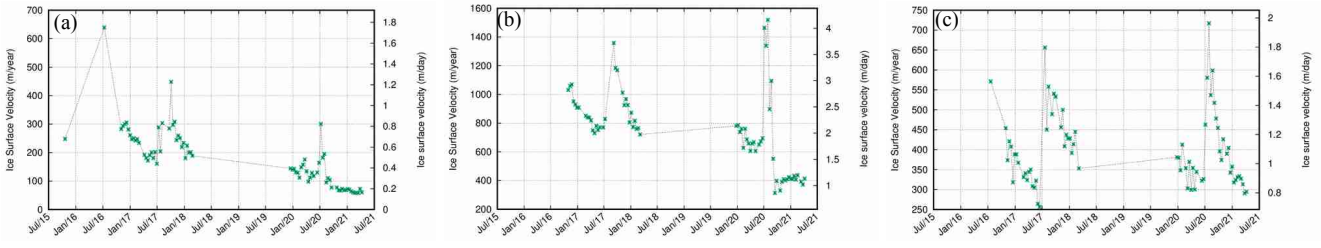

Figure 10: Franz-Josef-Land: time series of Sentinel-1 velocity for (a) Simony Glacier on McClintock Island (mean 183 m/a, mean summer 226 m/a (+23.8%), mean winter 174 m/a (-4.7%)), (b) west-oriented glacier of the Tyndal Ice Cap on Hall Island (mean 757 m/a, mean summer 922 m/a (+21.8%), mean winter 706 m/a (-6.7%)) and (c) Moscow Ice Cap Glacier 3 (mean 400 m/a, mean summer 490 m/a (+22.6%), mean winter 397 m/a (-7.6%)).

5.1.3 Severnaya Zemlya

On Severnaya Zemlya, the very prominent surging glacier on Vavilov Ice Cap has a decreasing trend of velocity since 2017, with strong summer speed-up events (Figure 11a). The glacier to the north of the Karpinsky Ice Cap, which had significantly larger velocities in 1991 compared to 2020/2021, now shows a decreasing trend of velocities, again with very pronounced summer speed-up events (Figure 11b). For the Academy of Sciences Ice Cap, we selected one glacier with a relatively constant velocity and short-time speed-up events, that are possibly not captured in 2017 and 2018, because of the lower quality of summer ice velocity maps compared to those from winter (Figure 11c). For the 17 glaciers analysed over Severnaya Zemlya with Sentinel-1 velocities larger than 100 m/a, the velocities in the winter period differed between -13% and +2% (average -5%) from the average annual velocities. The velocities in the summer period differed between +27% and -1% (average +11%) from the average annual velocities.

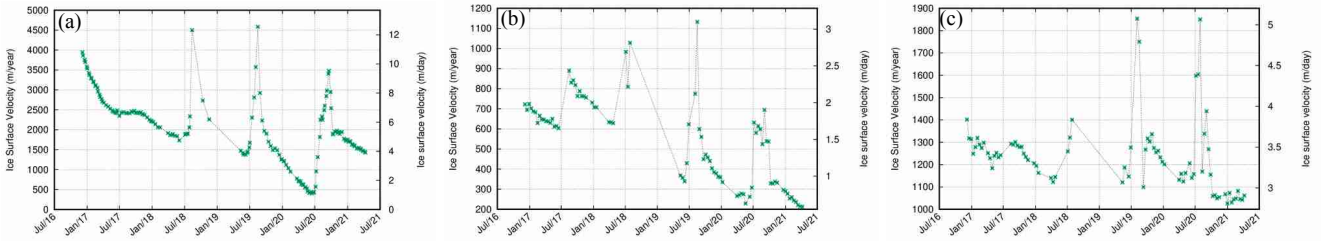

Figure 11: Severnaya Zemlya: time series of Sentinel-1 velocity for (a) Vavilov Ice Cap (mean 2062 m/a, mean summer 2117 m/a (+2.6%), mean winter 2021 m/a (-2.0%)), (b) north of the Karpinsky Ice Cap (mean 541 m/a, mean

https://doi.org/10.5194/essd-2022-44
Preprint. Discussion started: 17 February 2022

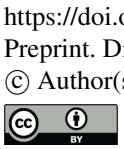

Open Access Earth System Science Data Discussions

summer 650 m/a (+20.1%), mean winter 488 m/a (-9.8%)) and (c) Academy of Sciences 6 (mean 1239 m/a, mean summer 1341 m/a (+8.2%), mean winter 1189 m/a (+4.0%)).

5.1.4 Svalbard

For Svalbard, we again show a few examples of time series for glaciers having distinctly different patterns. Over this region, there are 12-day acquisitions from both Sentinel-1A/B satellites, and in general the time-series are denser than over the Russian High Arctic. Basin 3 has a decreasing trend of velocity since 2015, after the peak of the surge, with strong summer speed-up events (Figure 12a), similar to what is observed for the surging outlet glacier on Vavilov Ice Cap over Severnaya Zemlya (Figure 7a). For Negribreen (Figure 12b), we observe a full surge cycle, with a very strong increase in winter 2017/2018, followed by a slowly decreasing trend with summer speed-up events. Kronebreen (Figure 12c) and Hornbreen (Figure 12d), on the other hand, do not show long-term changes, but strong velocity peaks in summer over Kronebreen and towards October-November over Hornbreen. For Hinlopenbreen (Figure 12e), the decrease of velocity after the summer speed-up is much slower than for Kronebreen and Hornbreen, lasting a few months. For Idabreen (Figure 12f), maximum velocities are reached during the winter, slowly decreasing to reach the minima in summer. For the 30 glaciers analysed in our study over Svalbard with Sentinel-1 velocities larger than 100 m/a, the velocities in the winter period differed between -13% and +14% (average 1%) compared to the average annual velocities. The velocities in the summer period differed between -33% and +46% (average -2%) compared to the average annual velocities. The variability of ice surface velocities over Svalbard, also graphically summarised in Figure 14, is much larger than over the Russian High Arctic. It is worth noting that in our list of glaciers, we included only two surging glaciers, Basin 3 and Negribreen.

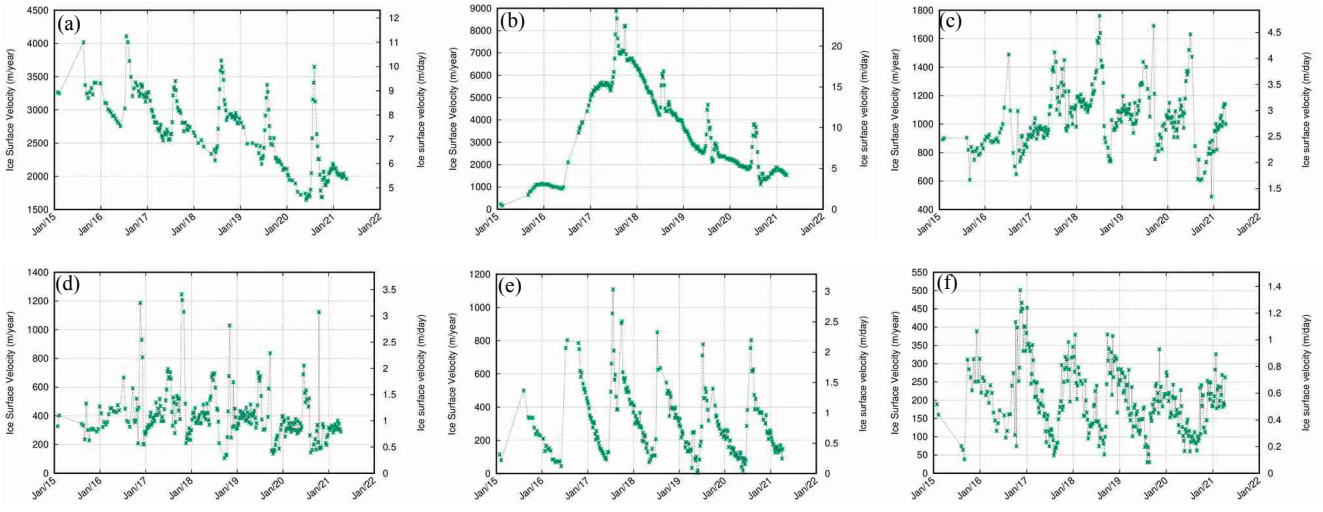

Figure 12: Svalbard: time series of Sentinel-1 velocity for (a) Basin 3 (mean 2650 m/a, mean summer 2787 m/a (+5.2%), mean winter 2537 m/a (-4.2%)), (b) Negribreen (mean 3148 m/a, mean summer 3668 m/a (+16.5%), mean winter 2905 m/a (-7.7%)), (c) Kronebreen (mean 1042 m/a, mean summer 1165 m/a (+11.8%), mean winter 1004 m/a

https://doi.org/10.5194/essd-2022-44
Preprint. Discussion started: 17 February 2022

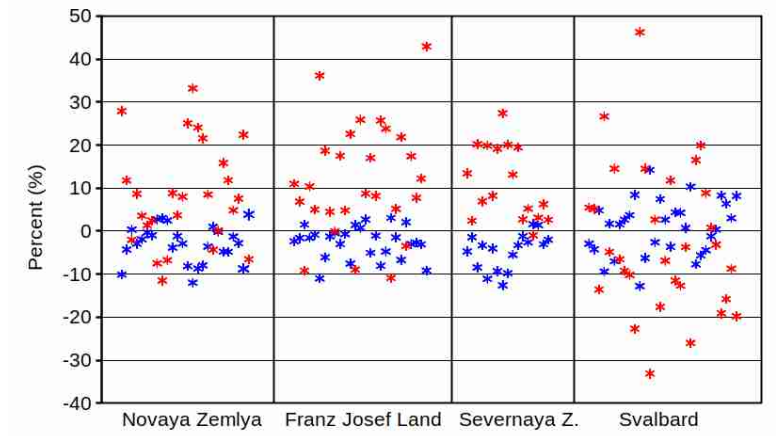

Figure 13: Differences between annual average ice surface velocity and winter (October-May, blue) and summer (June-September, red) averages for the glaciers analysed in our four study regions.

5.2 Interpretation of the long-term trends

We observed a general increase of winter velocities from the 1990's in the Eastern Arctic, along with a retreat of glacier fronts. Notable exceptions to this general pattern are surges, which are widespread over Svalbard but rarely found in the other three study regions. Indeed, for a couple of glaciers on Novaya Zemlya (e.g. Figures 9c), three glaciers on Severnaya Zemlya (e.g. Figures 11a, 11b) and more than ten glaciers on Svalbard (e.g. Figures 12a and 12b, the others not shown in this contribution but listed e.g., in Leclercq et al. (2021)), intra-annual trends in the Sentinel-1 ice surface velocity time-series dominate over inter-annual variability. Surges were not detected with our 1990's data. Few examples of surging glaciers as found in the literature (e.g., Monacobreen (Luckman et al., 2002) and Fridtjovbreen (Murray et al., 2003)) are missed, because they were asynchronous with our JERS-1 data coverage. At present, many more surging glaciers are observed over Svalbard than in the 1990's (Morris et al., 2020), making the interpretation of the long-term variability of ice surface velocity over this region challenging. It is expected that with the continued global temperature increase, the variability in the way glaciers respond to climate change will further increase. Some glaciers feature dynamic instabilities and discharge large amounts of ice, while others become dynamically less active and exhibit moderate rates of mass loss. As dynamic instabilities allow for larger, more rapid ice mass loss than surface melt, it is expected that ice discharge into the oceans will increase. Characteristic patterns of time series of ice surface velocities over dynamic instabilities will be analysed in future work.

https://doi.org/10.5194/essd-2022-44
Preprint. Discussion started: 17 February 2022

The dynamic response of land ice to climate forcing constitutes the main uncertainty in global sea level projections for the next century (Church et al., 2013; Martin and Adcroft, 2010). To address this knowledge gap, observations of the relative contribution of both surface mass balance and ice dynamics to the global mass losses are necessary. Using seven years of CryoSat-2 swath interferometric altimetry, Tepes et al. (2021) tracked changes in the volume of Arctic glaciers and ice caps and partitioned their losses into signals associated to atmospheric processes and glacier dynamics. They concluded that while surface ablation is responsible for 87% of losses across the Arctic, dynamic imbalance is increasing in the Barents and Kara Sea regions, where it now accounts for 43% of total ice loss. The persistent incursion of warm North Atlantic Ocean water into the Arctic Ocean, associated with a northward shift of Atlantic climate, is thought to have a direct impact on sea ice extent and tidewater glacier dynamics (McMillan et al., 2014; Polyakov et al., 2017; Barton et al., 2018). However, the respective role of internal processes, commonly ascribed to glacier surges, and external climatic forcing in driving these dynamic instabilities remains largely unclear (McMillan et al., 2014; Dunse et al., 2015). Quantifying calving fluxes to the ocean, composed of ice discharge to the ocean and marine-terminus retreat under the assumption of negligible melting and sublimation for grounded tidewater termini, is important to partition the causes of glacier mass loss. In order to quantify the regional decadal average calving flux, spatially and temporally consistent datasets of ice surface velocity are required together with consistent datasets of glacier ice thickness and terminus position (Kochtitzky et al., submitted). Our mosaics of winter ice surface velocities for the 1990's over the Eastern Arctic, with uncertainties of generally less than ±20 m/a, can support the assessment of the past regional decadal average calving flux for this region.

6 Conclusions

We computed nearly complete mosaics of winter ice surface velocities over the Eastern Arctic from the 1990's, presented long-term trends compared to results from ALOS-1 PALSAR-1 in winter 2008-2011 and Sentinel-1 in winter 2020/2021, and analysed the seasonal variability from Sentinel-1 data to infer the representativeness of winter velocities compared to annual averages. In most of the cases, winter velocities are a good representative of mean annual velocities, as seasonal fluctuations are relatively small for non-surging glaciers, with an underestimation of less than 10%, in particular over the Russian High Arctic. Summer velocities, on the other hand, can be significantly larger than the annual mean. Additionally, there are strong, short-time speed-up events during the summer period for many glaciers. We conclude that winter velocities give a better idea of long-term trends in speed, even if the spatial extend of the summer acceleration events, which can also be subject to long-term changes, is missed. Available ice surface velocity products based on Landsat-8 optical data such as GoLive, which also provide regularly updated scene-pair velocity fields, are limited to periods of solar illumination, therefore missing the winter season. As we showed, these data are more subject to summer speed-up events and thus less suited to analyse long-term trends in velocity. In addition, these products are less accurate in the very slow-moving accumulation areas, as these regions are difficult for optical feature tracking due to low-feature surfaces. Best approaches to integrate results derived from satellite SAR and optical missions still need to be further investigated.

https://doi.org/10.5194/essd-2022-44
Preprint. Discussion started: 17 February 2022

One of the crucial lessons learned from previous research on partitioning the causes of glacier mass loss is a severe problem with glacier velocity data and uncertainty of the calving flux estimation coming from this source. For an improved glacier monitoring strategy in the Eastern Arctic from Sentinel-1 SAR data, 6 days repeat is better suited than 12 days to retrieve high quality data, because time-series used to study dynamic instabilities are denser and the effects of ice and snow melting are less severe. In addition, acquisition gaps as occurred in 2018 and 2019 over Franz-Josef-Land should be avoided, as the Sentinel-1 time-series over this region (Figure 10) are of arduous interpretation. The spatial resolution of the IW Sentinel-1 SAR data (Table 1) is not optimal for studying ice surface velocity of Arctic glaciers and ice caps, but still acceptable as a compromise to the global acquisition strategy. Future L-band SAR missions such as NISAR (https://nisar.jpl.nasa.gov; last access: 7 September 2021), ALOS-4 (https://global.jaxa.jp/projects/sat/alos4; last access: 7 September 2021) or ROSE-L (https://www.esa.int/Our_Activities/Observing_the_Earth/Copernicus/Candidate_missions; last access: 7 September 2021) can complement the Sentinel-1 results.

Data availability

Output data

The ice surface velocity data set for the 1990's over the Eastern Arctic from satellite SAR data can be downloaded from https://doi.pangaea.de/10.1594/PANGAEA.938381 (Strozzi et. al. 2021).

Input data

JERS-1 SAR data are available from ESA as SLC at https://tpm-ds.eo.esa.int/socat/JERS1-SLC (last access: 6 September 2021) and from JAXA as RAW at https://gportal.jaxa.jp/gpr (last access: 6 September 2021). ERS-1/2 SAR data are available from ESA as RAW at http://esar-ds.eo.esa.int/socat/SAR_IM__0P_Scenes (last access: 6 September 2021). ALOS-1 PALSAR-1 RAW data are available from ESA at http://alos-ds.eo.esa.int/socat/ALOS_PALSAR_FBS_RAW_0P (last access: 6 September 2021), JAXA at https://gportal.jaxa.jp/gpr (last access: 6 September 2021), and ASF at https://search.asf.alaska.edu (last access: 6 September 2021). Sentinel-1 IW SLC data are available from Copernicus at https://scihub.copernicus.eu (last access: 6 September 2021).

The global TanDEM-X DEM at 3 arc second resolution is available at https://download.geoservice.dlr.de/TDM90 (last access: 6 September 2021). The digital elevation data derived from Soviet Union topographic maps of 1:100,000 and 1:200,000 scale are available at http://viewfinderpanoramas.org (last access: 6 September 2021).

The glacier outlines from summer satellite imagery spanning the period 2000-2010 for the Russian High Arctic (Moholdt et al., 2012) and Svalbard (Nuth et al., 2013) are available from the GLIMS glacier database at https://www.glims.org (last access: 6 September 2021). Glacier outlines between 2013 and 2016 over Novaya Zemlya (Rastner et al., 2017) and from 2016 for Franz-Josef-Land (unpublished) are available from the GLIMS glacier database at https://www.glims.org (last

https://doi.org/10.5194/essd-2022-44
Preprint. Discussion started: 17 February 2022

access: 6 September 2021). Glacier outlines from 2017 and 2018 for Svalbard (unpublished) can be provided upon request by the authors.

Author contributions

T.St., A.K. and F.P. designed the experiments; T.St. and A.W. processed most of the satellite SAR images, T.Sc. contributed with the analysis of the ERS-1/2 InSAR data over Svalbard; T.St. led the writing of the paper; all authors analysed the results and contributed to the redaction of the paper.

Acknowledgments

The research leading to these results received funding from the European Space Agency (ESA) within the Glaciers CCI project (Grant 4000127593/19/I-NB) and the EarthExplorer10 Harmony Mission Advisory Group, and from the Norwegian Space Centre project Copernicus Glacier Service for Norway (NIT.06.15.5). The study is a contribution to the Svalbard Integrated Arctic Earth Observing System SIOS. A sincere thanks to Nina Jones for her diligent proofreading of this article.

References

Barton, B. I., Lenn, Y.-D., and Lique, C.: Observed Atlantification of the Barents Sea Causes the Polar Front to Limit the Expansion of Winter Sea Ice, 48, 1849–1866, https://doi.org/10.1175/JPO-D-18-0003.1, 2018.

Benn, D. I., Jones, R. L., Luckman, A., Fürst, J. J., Hewitt, I., and Sommer, C.: Mass and enthalpy budget evolution during the surge of a polythermal glacier: a test of theory, J. Glaciol., 65, 717–731, https://doi.org/10.1017/jog.2019.63, 2019.

Blaszczyk, M., Jania, J., and Hagen, J.O.: Tidewater glaciers of Svalbard: Recent changes and estimates of calving fluxes. Polish Polar Research, 30(2), 85–142, 2009.

Burgess, E. W., Forster, R. R., and Larsen, C. F.: Flow velocities of Alaskan glaciers, Nat Commun, 4, 2146, https://doi.org/10.1038/ncomms3146, 2013.

Church, J.A., et al. Climate change 2013: The physical science basis. In: Contribution of Working Group I to the Fifth Assessment Report of the Intergovernmental Panel on Climate Change (IPCC). Cambridge Univ. Press, Cambridge, 2013.

Dehecq, A., Gourmelen, N., and Trouve, E.: Deriving large-scale glacier velocities from a complete satellite archive: Application to the Pamir–Karakoram–Himalaya, Remote Sensing of Environment, 162, 55–66, https://doi.org/10.1016/j.rse.2015.01.031, 2015.

Dowdeswell, J. A., Bassford, R. P., Gorman, M. R., Williams, M., Glazovsky, A. F., Macheret, Y. Y., Shepherd, A. P., Vasilenko, Y. V., Savatyuguin, L. M., Hubberten, H.-W., and Miller, H.: Form and flow of the Academy of Sciences Ice

https://doi.org/10.5194/essd-2022-44
Preprint. Discussion started: 17 February 2022

Cap, Severnaya Zemlya, Russian High Arctic, J. Geophys. Res., 107, EPM 5-1-EPM 5-15, https://doi.org/10.1029/2000JB000129, 2002.

Dunse, T., Schellenberger, T., Hagen, J. O., Kääb, A., Schuler, T. V., and Reijmer, C. H.: Glacier-surge mechanisms promoted by a hydro-thermodynamic feedback to summer melt, The Cryosphere, 9, 197–215, https://doi.org/10.5194/tc-9-197-2015, 2015.

Fahnestock, M., Scambos, T., Moon, T., Gardner, A., Haran, T., and Klinger, M.: Rapid large-area mapping of ice flow using Landsat 8, Remote Sensing of Environment, 185, 84–94, https://doi.org/10.1016/j.rse.2015.11.023, 2016.

Flink, A. E., Noormets, R., Kirchner, N., Benn, D. I., Luckman, A., and Lovell, H.: The evolution of a submarine landform record following recent and multiple surges of Tunabreen glacier, Svalbard, Quaternary Science Reviews, 108, 37–50, https://doi.org/10.1016/j.quascirev.2014.11.006, 2015.

Friedl, P., Seehaus, T., and Braun, M.: Global time series and temporal mosaics of glacier surface velocities, derived from Sentinel-1 data, 1–33, https://doi.org/10.5194/essd-2021-106, 2021.

Gardner, A. S., Moholdt, G., Scambos, T., Fahnstock, M., Ligtenberg, S., van den Broeke, M., and Nilsson, J.: Increased West Antarctic and unchanged East Antarctic ice discharge over the last 7 years, The Cryosphere, 12, 521–547, https://doi.org/10.5194/tc-12-521-2018, 2018.

Glazovsky, A., Bushueva, I., and Nosenko, G., “Slow” surge of the Vavilov Ice Cap, Severnaya Zemlya. In Proceedings ofthe IASC Workshop on the Dynamics and Mass Balance of Arctic Glaciers, Obergurgl, Austria, 23–25 March 2015.

Hugonnet, R., McNabb, R., Berthier, E., Menounos, B., Nuth, C., Girod, L., Farinotti, D., Huss, M., Dussaillant, I., Brun, F., and Kääb, A.: Accelerated global glacier mass loss in the early twenty-first century, Nature, 592, 726–731, https://doi.org/10.1038/s41586-021-03436-z, 2021.

Kochtitzky, W., Copland, L., Van Wychen, W., Hugonnet., R., Hock, R., Dowdeswell, J., Benham, T., Strozzi, T., Glazovsky, A., Lavrentiev, I., Rounce, D., Millan, R., Cook, A., Dalton, A., Jiskoot, H., Cooley, J., Jania, J., and Navarro, F., Frontal ablation, the unquantified mass loss of marine-terminating glaciers, 2000-2020, Nature Communications, submitted.

Leclercq, P. W., Kääb, A., and Altena, B.: Brief Communication: Detection of glacier surge activity using cloud computing of Sentinel-1 radar data, The Cryosphere Discuss. [preprint], https://doi.org/10.5194/tc-2021-89, 2021.

Luckman, A., Murray, T., and Strozzi, T.: Surface flow evolution throughout a glacier surge measured by satellite radar interferometry, Geophys. Res. Lett., 29(23), 10.1–10.4, https://doi.org/10.1029/2001GL014570, 2002.

Martin, T. and Adcroft, A.: Parameterizing the fresh-water flux from land ice to ocean with interactive icebergs in a coupled climate model, Ocean Modelling, 34, 111–124, https://doi.org/10.1016/j.ocemod.2010.05.001, 2010.

McMillan, M., Shepherd, A., Gourmelen, N., Dehecq, A., Leeson, A., Ridout, A., Flament, T., Hogg, A., Gilbert, L., Benham, T., van den Broeke, M., Dowdeswell, J. A., Fettweis, X., Noël, B., and Strozzi, T.: Rapid dynamic activation of a marine-based Arctic ice cap: Ice cap dynamic activation, Geophys. Res. Lett., 41, 8902–8909, https://doi.org/10.1002/2014GL062255, 2014.

https://doi.org/10.5194/essd-2022-44
Preprint. Discussion started: 17 February 2022

Moholdt, G., Wouters, B., and Gardner, A. S.: Recent mass changes of glaciers in the Russian High Arctic, 39, https://doi.org/10.1029/2012GL051466, 2012.

Morris, A., Moholdt, G., and Gray, L.: Spread of Svalbard Glacier Mass Loss to Barents Sea Margins Revealed by CryoSat-2, J. Geophys. Res. Earth Surf., 125, https://doi.org/10.1029/2019JF005357, 2020.

Murray, T., Luckman, A., Strozzi, T., and Nuttall, A.-M.: The initiation of glacier surging at Fridtjovbreen, Svalbard, Ann. Glaciol., 36, 110–116, https://doi.org/10.3189/172756403781816275, 2003.

Nagler, T., Rott, H., Hetzenecker, M., Wuite, J., and Potin, P.: The Sentinel-1 Mission: New Opportunities for Ice Sheet Observations, 7, 9371–9389, https://doi.org/10.3390/rs70709371, 2015.

Nuth, C., Kohler, J., König, M., von Deschwanden, A., Hagen, J. O., Kääb, A., Moholdt, G., and Pettersson, R.: Decadal changes from a multi-temporal glacier inventory of Svalbard, The Cryosphere, 7, 1603–1621, https://doi.org/10.5194/tc-7-1603-2013, 2013.

Nuth, C., Gilbert, A., Köhler, A., McNabb, R., Schellenberger, T., Sevestre, H., Weidle, C., Girod, L., Luckman, A., and Kääb, A.: Dynamic vulnerability revealed in the collapse of an Arctic tidewater glacier, Sci Rep, 9, 5541, https://doi.org/10.1038/s41598-019-41117-0, 2019.

Paul, F., Bolch, T., Kääb, A., Nagler, T., Nuth, C., Scharrer, K., Shepherd, A., Strozzi, T., Ticconi, F., Bhambri, R., Berthier, E., Bevan, S., Gourmelen, N., Heid, T., Jeong, S., Kunz, M., Lauknes, T. R., Luckman, A., Merryman Boncori, J. P., Moholdt, G., Muir, A., Neelmeijer, J., Rankl, M., VanLooy, J., and Van Niel, T.: The glaciers climate change initiative: Methods for creating glacier area, elevation change and velocity products, Remote Sensing of Environment, 162, 408–426, https://doi.org/10.1016/j.rse.2013.07.043, 2015.

Paul, F., Bolch, T., Briggs, K. Kääb, A., McMillan, M, McNabb, R., Nagler, T., Nuth, C., Rastner, P., Strozzi, T. and Wuite, J.: Error sources and guidelines for quality assessment of glacier area, elevation change, and velocity products derived from satellite data in the Glaciers_cci project, Remote Sensing of Environment, 203, 256-275, https://doi.org/10.1016/j.rse.2017.08.038, 2017.Paterson, W. S. B.: The physics of glaciers, 3rd ed., Pergamon, Oxford, OX, England ; Tarrytown, N.Y., U.S.A, 480 pp., 1994.

Pohjola, V. A., Christoffersen, P., Kolondra, L., Moore, J. C., Pettersson, R., Schäfer, M., Strozzi, T., and Reijmer, C. H.: Spatial distribution and change in the surface ice velocity field of vestfonna ice cap, Nordaustlandet, Svalbard, 1995-2010 using geodetic and satellite interferometry data, Geografiska Annaler Series A-Physical Geography, 93, 323–335, https://doi.org/10.1111/j.1468-0459.2011.00441.x, 2011.

Polyakov, I. V., Pnyushkov, A. V., Alkire, M. B., Ashik, I. M., Baumann, T. M., Carmack, E. C., Goszczko, I., Guthrie, J., Ivanov, V. V., Kanzow, T., Krishfield, R., Kwok, R., Sundfjord, A., Morison, J., Rember, R., and Yulin, A.: Greater role for Atlantic inflows on sea-ice loss in the Eurasian Basin of the Arctic Ocean, Science, 356, 285–291, https://doi.org/10.1126/science.aai8204, 2017.

Rastner, P., Strozzi, T., and Paul, F.: Fusion of Multi-Source Satellite Data and DEMs to Create a New Glacier Inventory for Novaya Zemlya, Remote Sensing, 9, 1122, https://doi.org/10.3390/rs9111122, 2017.

https://doi.org/10.5194/essd-2022-44
Preprint. Discussion started: 17 February 2022

Scambos, T., Fahnestock, M., Moon, T., Gardner, A., and Klinger, M., Global Land Ice Velocity Extraction from Landsat 8 (GoLIVE), Version 1, Boulder, Colorado USA, NSIDC: National Snow and Ice Data Center, http://dx.doi.org/10.7265/N5ZP442B, 2016.

Schellenberger, T., Dunse, T., Kääb, A., Schuler, T. V., Hagen, J. O., and Reijmer, C. H.: Multi-year surface velocities and sea-level rise contribution of the Basin-3 and Basin-2 surges, Austfonna, Svalbard, Glaciers, The Cryosphere Discuss., https://doi.org/10.5194/tc-2017-5, 2017.

Schuler, T. V., Kohler, J., Elagina, N., Hagen, J. O. M., Hodson, A. J., Jania, J. A., Kääb, A. M., Luks, B., Małecki, J., Moholdt, G., Pohjola, V. A., Sobota, I., and Van Pelt, W. J. J.: Reconciling Svalbard Glacier Mass Balance, Front. Earth Sci., 8, 156, https://doi.org/10.3389/feart.2020.00156, 2020.

Strozzi, T., Luckman, A., Murray, T., Wegmuller, U., and Werner, C. L.: Glacier motion estimation using SAR offset-tracking procedures, IEEE Trans. Geosci. Remote Sensing, 40, 2384–2391, https://doi.org/10.1109/TGRS.2002.805079, 2002.

Strozzi, T., Kouraev, A., Wiesmann, A., Wegmüller, U., Sharov, A., and Werner, C.: Estimation of Arctic glacier motion with satellite L-band SAR data, Remote Sensing of Environment, 112, 636–645, https://doi.org/10.1016/j.rse.2007.06.007, 2008.

Strozzi, T., Paul, F., Wiesmann, A., Schellenberger, T., and Kääb, A.: Circum-Arctic Changes in the Flow of Glaciers and Ice Caps from Satellite SAR Data between the 1990s and 2017, Remote Sensing, 9, 947, https://doi.org/10.3390/rs9090947, 2017.

Strozzi, T., Wiesmann, A., Kääb, A., Schellenberger, T., Paul, F.: Ice Surface Velocity in the Eastern Arctic from Past Spaceborne SAR Data. PANGAEA, https://doi.org/10.1594/PANGAEA.938381, 2021.

Sund, M., Lauknes, T. R., and Eiken, T.: Surge dynamics in the Nathorstbreen glacier system, Svalbard, The Cryosphere, 8, 623–638, https://doi.org/10.5194/tc-8-623-2014, 2014.

Tepes, P., Gourmelen, N., Nienow, P., Tsamados, M., Shepherd, A., and Weissgerber, F.: Changes in elevation and mass of Arctic glaciers and ice caps, 2010–2017, Remote Sensing of Environment, 261, 112481, https://doi.org/10.1016/j.rse.2021.112481, 2021.

Wegmüller, U., Werner, C., Strozzi, T., and Wiesmann, A.: Ionospheric electron concentration effects on SAR and INSAR, Proceedings of IGARSS, Denver (USA), https://doi.org/10.1109/IGARSS.2006.956, 31 July- 4 August 2006.

Werner, C., Wegmuller, U., Strozzi, T., and Wiesmann, A.: Precision estimation of local offsets between pairs of SAR SLCs and detected SAR images, Proc. IEEE Int. Geosci. Remote Sens. Symp. (IGARSS), Seoul, Korea, 4803–4805, https://doi.org/10.1109/IGARSS.2005.1526747, 2005.

Willis, M. J., Melkonian, A. K., and Pritchard, M. E.: Outlet glacier response to the 2012 collapse of the Matusevich Ice Shelf, Severnaya Zemlya, Russian Arctic, J. Geophys. Res. Earth Surf., 120, 2040–2055, https://doi.org/10.1002/2015JF003544, 2015.

https://doi.org/10.5194/essd-2022-44
Preprint. Discussion started: 17 February 2022

Willis, M. J., Zheng, W., Durkin, W. J., Pritchard, M. E., Ramage, J. M., Dowdeswell, J. A., Benham, T. J., Bassford, R. P., Stearns, L. A., Glazovsky, A. F., Macheret, Y. Y., and Porter, C. C.: Massive destabilization of an Arctic ice cap, Earth and Planetary Science Letters, 502, 146–155, https://doi.org/10.1016/j.epsl.2018.08.049, 2018.

Wouters, B., Gardner, A. S., and Moholdt, G.: Global Glacier Mass Loss During the GRACE Satellite Mission (2002-2016), Front. Earth Sci., 7, 96, https://doi.org/10.3389/feart.2019.00096, 2019.

Zemp, M., Huss, M., Thibert, E., Eckert, N., McNabb, R., Huber, J., Barandun, M., Machguth, H., Nussbaumer, S. U., Gärtner-Roer, I., Thomson, L., Paul, F., Maussion, F., Kutuzov, S., and Cogley, J. G.: Global glacier mass changes and their contributions to sea-level rise from 1961 to 2016, Nature, 568, 382–386, https://doi.org/10.1038/s41586-019-1071-0, 2019.

Zheng, W., Pritchard, M. E., Willis, M. J., and Stearns, L. A.: The Possible Transition From Glacial Surge to Ice Stream on Vavilov Ice Cap, Geophys. Res. Lett., 46, 13892–13902, https://doi.org/10.1029/2019GL084948, 2019.

https://doi.org/10.5194/essd-2022-44
Preprint. Discussion started: 17 February 2022

Open Access Earth System Science Data Discussions

Appendix A. Satellite data.

Table A1. JERS-1 SAR data over Novaya Zemlya.

Track_Frame	Orbit	Date 1	Date 2	Baseline (m)	Interval (d)	Stdev (m/a)	Percent (%)
0239_0177	DESC	19980209	19980325	392.6	44	11.46	83.91
0239_0176	DESC	19980209	19980325	401.1	44	13.33	39.06
0239_0175	DESC	19980209	19980325	409.8	44	13.69	23.35
0235_0177	DESC	19980205	19980321	363.6	44	7.77	93.04
0235_0176	DESC	19980205	19980321	373.9	44	6.76	94.28
0235_0175	DESC	19980205	19980321	384.2	44	9.83	90.97
0235_0174	DESC	19980205	19980321	394.5	44	19.89	88.78
0235_0173	DESC	19980205	19980321	404.8	44	29.67	79.87
0235_0172	DESC	19980205	19980321	415.2	44	41.60	73.36
0231_0174	DESC	19980201	19980317	400.5	44	11.58	79.90
0231_0173	DESC	19980201	19980317	406.9	44	16.61	90.32
0231_0172	DESC	19980201	19980317	413.2	44	25.21	86.61
0228_0173	DESC	19980129	19980314	347.5	44	23.94	81.51
0228_0172	DESC	19980129	19980314	353.8	44	17.10	87.55
0228_0171	DESC	19980129	19980314	360.1	44	41.28	67.08
0220_0172	DESC	19980121	19980306	-75.7	44	18.05	64.96
0220_0171	DESC	19980121	19980306	-52.6	44	20.33	87.21
0220_0170	DESC	19980121	19980306	-33.9	44	12.39	85.19
0225_0172	DESC	19980126	19980311	521.1	44	20.55	86.60
0225_0171	DESC	19980126	19980311	520.7	44	33.96	80.77
0225_0170	DESC	19980126	19980311	520.2	44	79.90	59.12

Table A2. ALOS-1 PALSAR-1 data over Novaya Zemlya.

Track_Frames	Orbit	Date 1	Date 2	Baseline (m)	Interval (d)	Stdev (m/a)	Percent (%)
523_1510-1520	ASC	20081211	20090126	723.4	46	33.48	88.94
513_1520-1530	ASC	20081225	20090209	844.1	46	31.89	93.68
535_1460-1490	ASC	20081231	20090215	850.4	46	9.95	92.01
527_1500-1510	ASC	20090102	20090217	765.9	46	27.11	93.48
519_1530-1540	ASC	20090104	20090219	725.2	46	27.13	92.49
525_1530-1540	ASC	20090114	20090301	707.6	46	33.08	94.50
517_1500-1520	ASC	20090116	20090303	697.4	46	27.28	94.16
509_1530-1540	ASC	20090118	20090305	709.6	46	44.31	92.06
539_1460	ASC	20090122	20090309	750.5	46	5.56	96.44

https://doi.org/10.5194/essd-2022-44
Preprint. Discussion started: 17 February 2022

Open Access Earth System Science Data Discussions

531_1480-1510	ASC	20100314	20100429	359.9	46	19.00	93.46

Table A3. Sentinel-1 data over Novaya Zemlya.

Track	Orbit	Date 1	Date 2	Baseline (m)	Interval (d)	Stdev (m/a)	Percent (%)
6	DESC	20210213	20210225	-66.7	12	43.63	97.26
50	DESC	20210204	20210216	36.5	12	25.23	96.51

Table A4. JERS-1 SAR data over Franz-Josef-Land.

Track_Frame	Orbit	Date 1	Date 2	Baseline (m)	Interval (d)	Stdev (m/a)	Percent (%)
0249_0161	DESC	19980106	19980219	192.4	44	9.39	77.48
0249_0162	DESC	19980106	19980219	186.0	44	13.89	93.86
0249_0163	DESC	19980106	19980219	179.6	44	34.64	93.41
0249_0164	DESC	19980106	19980219	173.1	44	31.93	87.16
0249_0165	DESC	19980106	19980219	166.5	44	15.51	74.87
0255_0161	DESC	19980112	19980225	-53.8	44	24.42	83.69
0255_0162	DESC	19980112	19980225	-74.0	44	23.3	85.87
0255_0163	DESC	19980112	19980225	-94.3	44	22.64	88.15
0255_0164	DESC	19980112	19980225	-114.3	44	18.29	90.07
0260_0161	DESC	19980302	19980529	1244.8	88	21.04	93.68
0260_0162	DESC	19980302	19980529	1309.0	88	15.65	89.58
0260_0163	DESC	19980302	19980529	1372.0	88	15.57	88.31
0260_0164	DESC	19980302	19980529	1435.8	88	15.15	94.43
0260_0165	DESC	19980302	19980529	1499.5	88	24.04	92.09
0270_0162	DESC	19980312	19980425	350.7	44	18.41	96.44
0270_0163	DESC	19980312	19980425	338.7	44	26.2	84.39
0270_0164	DESC	19980312	19980425	326.7	44	26.8	89.66
0267_0163	DESC	19960404	19960518	529.7	44	24.09	93.70
0267_0164	DESC	19960404	19960518	556.4	44	23.72	92.86
0270_0163	DESC	19960407	19960521	528.7	44	27.3	56.30
0279_0163	DESC	19971109	19971223	979.6	44	27.64	75.08

Table A5. ERS-1 SAR data over Franz-Josef-Land.

Track_Frame	Orbit	Date 1	Date 2	Baseline (m)	Interval (d)	Stdev (m/a)	Percent (%)
36_1944	DESC	19911108	19911117	79.7	9	52.69	94.92
40_1647	ASC	19911012	19911021	219.0	9	53.22	74.29
40_1647	ASC	19911021	19911102	208.8	12	34.67	82.51

https://doi.org/10.5194/essd-2022-44
Preprint. Discussion started: 17 February 2022

Open Access Earth System Science Data Discussions

Table A6. ALOS-1 PALSAR-1 data over Franz-Josef-Land.

Track_Frames	Orbit	Date 1	Date 2	Baseline (m)	Interval (d)	Stdev (m/a)	Percent (%)
526_1610-1630	ASC	20101222	20110206	824.4	46	31.14	92.92
522_1610-1620	ASC	20110302	20110417	593.5	46	18.72	92.50

Table A7. Sentinel-1 SAR data over Franz-Josef-Land.

Track	Orbit	Date 1	Date 2	Baseline (m)	Interval (d)	Stdev (m/a)	Percent (%)
36	DESC	20210110	20210122	-60.5	12	32.59	94.0689
167	DESC	20210131	20210212	54.0	12	33.49	97.7057

Table A8. ERS-1 data over Severnaya Zemlya.

Track_Frame	Orbit	Date 1	Date 2	Baseline (m)	Interval (d)	Stdev (m/a)	Percent (%)
10_1642	ASC	19920302	19920320	361.7	18	41.35	3.11
10_1658	ASC	19920302	19920320	357.4	18	64.98	38.54
10_1614	ASC	19920207	19920219	143.0	12	69.12	81.95
10_1629	ASC	19920207	19920219	137.1	12	44.87	94.33
10_1642	ASC	19920207	19920219	129.7	12	19.11	91.23
39_1603	ASC	19911018	19911102	365.7	15	50.64	45.42
39_1611	ASC	19911018	19911102	391.2	15	45.85	72.83
39_1629	ASC	19911018	19911102	416.7	15	36.21	39.21

Table A9. Sentinel-1 data over Severnaya Zemlya.

Track	Orbit	Date 1	Date 2	Baseline (m)	Interval (d)	Stdev (m/a)	Percent (%)
49	DESC	20201218	20201230	70.7	12	24.87	90.62
49	DESC	20210123	20210204	-25.4	12	24.42	91.24
5	DESC	20201215	20201227	-57.6	12	21.80	92.26
5	DESC	20210213	20210225	-64.6	12	22.93	89.61

Table A10. JERS-1 data over Svalbard.

Track_Frames	Orbit	Date 1	Date 2	Baseline (m)	Interval (d)	Stdev (m/a)	Percent (%)
0293_0164	DESC	19971123	19980106	916.1	44	0.00	85.09
0306_0169	DESC	19971206	19980119	809.8	44	19.22	71.20
0306_0168	DESC	19971206	19980119	801.4	44	14.49	82.19
0306_0167	DESC	19971206	19980119	792.1	44	0.00	0.52
0306_0166	DESC	19971206	19980119	783.5	44	0.00	53.80
0306_0165	DESC	19971206	19980119	775.0	44	21.55	65.85

https://doi.org/10.5194/essd-2022-44
Preprint. Discussion started: 17 February 2022

0306_0164	DESC	19971206	19980119	766.3	44	49.47	83.40
0308_0164	DESC	19971208	19980121	548.3	44	32.75	82.95
0308_0165	DESC	19971208	19980121	548.2	44	20.32	82.19
0308_0166	DESC	19971208	19980121	547.9	44	0.00	74.55
0308_0167	DESC	19971208	19980121	547.6	44	28.90	59.01
0308_0168	DESC	19971208	19980121	547.3	44	14.20	77.82
0308_0169	DESC	19971208	19980121	546.8	44	15.32	79.40
0312_0164	DESC	19971212	19980125	323.7	44	11.67	85.75
0312_0165	DESC	19971212	19980125	306.9	44	8.43	82.31
0312_0166	DESC	19971212	19980125	290.2	44	10.43	75.17
0312_0167	DESC	19971212	19980125	273.1	44	16.07	65.54
0312_0168	DESC	19971212	19980125	256.7	44	19.99	38.73
0312_0169	DESC	19971212	19980125	239.6	44	49.90	48.21
0312_0170	DESC	19971212	19980125	222.7	44	64.26	48.37
0312_0171	DESC	19971212	19980125	205.6	44	64.55	66.12
0314_0167	DESC	19940205	19940321	804.6	44	14.19	93.70
0314_0166	DESC	19940205	19940321	809.6	44	14.53	101.87
0314_0170	DESC	19971214	19980127	261.0	44	34.47	77.07
0314_0169	DESC	19971214	19980127	270.8	44	19.96	80.71
0314_0168	DESC	19971214	19980127	280.5	44	21.60	78.70
0314_0167	DESC	19971214	19980127	290.2	44	14.79	76.72
0314_0166	DESC	19971214	19980127	299.9	44	12.53	74.74
0314_0165	DESC	19971214	19980127	309.6	44	8.83	84.45
0314_0164	DESC	19971214	19980127	319.1	44	8.21	88.91
0316_0170-68	DESC	19940323	19940506	352.1	44	14.64	51.66
0316_0166-64	DESC	19940323	19940506	360.2	44	21.99	84.47
0328_0167	DESC	19971228	19980210	11.5	44	9.69	71.59
0328_0166	DESC	19971228	19980210	-9.1	44	18.79	88.30
0328_0165	DESC	19971228	19980210	-24.6	44	15.07	90.16
0328_0167	DESC	19980210	19980326	343.1	44	24.72	78.62
0328_0166	DESC	19980210	19980326	358.1	44	21.76	88.94
0328_0165	DESC	19980210	19980326	373.7	44	30.18	72.05
0330_0167	DESC	19971116	19971230	1247.2	44	30.75	78.57
0330_0166	DESC	19971116	19971230	1220.5	44	26.84	84.11
0330_0165	DESC	19971116	19971230	1193.2	44	18.16	87.14

https://doi.org/10.5194/essd-2022-44
Preprint. Discussion started: 17 February 2022

Open Access Earth System Science Data Discussions

Table A11. ERS-1/2 InSAR data over Svalbard.

Track	Frames	Orbit	Date 1	Date 2	Baseline (m)	Interval (d)
70	1629	ASC	19951215	19951216	60	1
70	1629	ASC	19960119	19960120	229	1
80	1959 – 1977	DESC	19951216	19951217	-48	1
80	1959 – 1977	DESC	19960120	19960121	205	1
199	1617 – 1635	ASC	19951224	19951225	141	1
199	1617 – 1635	ASC	19960128	19960129	117	1
495	953 – 1971	DESC	19951210	19951211	30	1
495	953 – 1971	DESC	19960114	19960115	46	1
42	1575	ASC	19971217	19971218	118	1
452	2025	DESC	19960321	19960322	32	1
185	1611	ASC	19951226	19951227	109	1
166	1989	DESC	19960405	19960406	12	1

Table A12. ERS-1 data over Svalbard.

Track_Frame	Orbit	Date 1	Date 2	Baseline (m)	Interval (d)	Stdev (m/a)	Percent (%)
23_1953	DESC	19920103	19920115	93.3	12	18.85	48.07
23_1971	DESC	19920103	19920115	75.4	12	24.37	64.72
23_1989	DESC	19920103	19920115	57.4	12	27.95	57.57
23_2007	DESC	19920103	19920115	39.5	12	28.65	72.15
23_2025	DESC	19920103	19920115	21.4	12	46.56	58.13

Table A13. ALOS-1 PALSAR-1 data over Svalbard.

Track_Frames	Orbit	Date 1	Date 2	Baseline (m)	Interval (d)	Stdev (m/a)	Percent (%)
576_1600-1620	ASC	20080105	20080220	971.0	46	7.95	72.35
583_1600-1610	ASC	20080201	20080318	677.5	46	8.89	95.36
586_1560	ASC	20101114	20110214	1420.9	92	12.60	60.39
586_1560-1570	ASC	20110104	20110219	872.3	46	3.67	91.80
595_1560-1570	ASC	20110114	20110301	748.3	46	15.98	93.11

Table A14. Sentinel-1 data over Svalbard.

Track	Orbit	Date 1	Date 2	Baseline (m)	Interval (d)	Stdev (m/a)	Percent (%)
14	ASC	20210120	20210201	50.2	12	13.59	94.37
174	ASC	20210131	20210212	55.7	12	13.32	89.79
174	ASC	20210206	20210212	84.0	6	21.74	96.62

https://doi.org/10.5194/essd-2022-44
Preprint. Discussion started: 17 February 2022

Open Access Earth System Science Data Discussions

Appendix B. Glacier's statistics.

Table B1. Novaya Zemlya: statistics for time series of Sentinel-1 velocity 2015-2021.

Name	Long.	Lat.	Mean Year	Max Year	Min Year	Mean Summer	Percent Summer	Mean Winter	Percent Winter
Severny_1	746764	8545276	396	1252	79	507	**27.9**	356	**-10.1**
Severny_2	741328	8530470	661	1034	428	739	**11.8**	632	**-4.3**
Severny_3	739259	8505718	676	1254	416	662	**-2.0**	679	**0.3**
Vize_4	714375	8498416	456	781	165	496	**8.7**	443	**-2.9**
Severny_5	706501	8485936	630	1030	312	652	**3.5**	617	**-1.9**
Severny_6	694115	8479524	470	1015	246	476	**1.3**	469	**-0.3**
Severny_7	689392	8475873	738	1017	461	756	**2.5**	731	**-1.0**
Severny_8	671672	8472142	627	907	346	580	**-7.5**	644	**2.7**
Severny_9	662782	8464880	838	1465	374	742	**-11.5**	864	**3.1**
Shokalskiy_10	650280	8460077	719	1064	445	671	**-6.8**	737	**2.5**
Chernyshev_11	605924	8440027	553	928	282	601	**8.8**	531	**-3.9**
Krayniy_Popov_12	580108	8426112	581	981	238	602	**3.7**	574	**-1.2**
Krivosheina_13	551729	8407070	690	1239	497	746	**8.0**	670	**-2.9**
Vilkitskiy_14	542025	8392240	440	1066	237	550	**25.1**	404	**-8.1**
Severny_15	537964	8386298	340	803	203	453	**33.2**	299	**-12.0**
Nordenskiold_16	528439	8360938	481	1100	297	597	**24.1**	439	**-8.7**
Glazov_17	502583	8348119	357	788	230	434	**21.6**	329	**-8.0**
Nizkiy_18	487264	8328771	235	427	170	256	**8.5**	227	**-3.6**
Severny_92	510353	8234169	162	260	90	155	**-4.3**	164	**1.0**
Severny_93	534855	8274953	118	225	21	118	**0.1**	117	**-0.2**
Severny_94	583790	8326135	277	1258	116	320	**15.8**	263	**-4.8**
Vylki_Shury_95	615505	8350781	250	435	189	280	**11.8**	238	**-4.8**
Severny_96	636103	8379058	441	592	285	462	**4.8**	435	**-1.3**
Moshchnyy_97	659380	8389476	388	600	236	417	**7.6**	377	**-2.8**
Severny_98	700615	8418170	212	451	37	260	**22.4**	194	**-8.8**
Severny_99	745978	8453055	159	592	23	149	**-6.6**	166	**3.9**

https://doi.org/10.5194/essd-2022-44
Preprint. Discussion started: 17 February 2022

Open Access Earth System Science Data Discussions

685 **Table B2. Franz-Josef-Land: statistics for time series of Sentinel-1 velocity 2015-2021.**

Name	Long.	Lat.	Mean Year	Max Year	Min Year	Mean Summer	Percent Summer	Mean Winter	Percent Winter
Brousilov_1	366902	8962633	369	545	230	409	**11,0**	360	**-2,4**
Brousilov_2	373548	8946717	398	648	256	426	**6,9**	392	**-1,6**
Brousilov_3	380278	8968170	239	596	55	217	**-9,2**	243	**1,5**
Brousilov_4	349663	8945647	236	341	87	261	**10,4**	232	**-1,6**
Champ	498831	8956263	138	292	36	145	**5,0**	137	**-0,9**
Chernysheva	554269	8882395	236	1130	133	321	**36,1**	209	**-11,0**
Forbes	523208	8977770	113	290	52	134	**18,7**	106	**-6,1**
Luigi	469416	8973739	158	406	8	165	**4,5**	156	**-1,3**
Moon_4	308002	8975620	303	585	151	302	**0,0**	301	**-0,5**
Moscow_1	515965	8902160	207	414	100	243	**17,5**	201	**-3,0**
Moscow_2	527584	8917124	237	384	83	248	**4,8**	235	**-0,7**
Moscow_3	515265	8933468	400	717	257	490	**22,6**	370	**-7,6**
Northbrook_2	387401	8883086	228	389	10	208	**-9,0**	231	**1,4**
Rudolph_Island_1	535877	9081462	207	1493	79	261	**25,9**	209	**0,7**
Rudolph_Island_2	528215	9074816	166	1016	21	180	**8,7**	170	**2,7**
Salisbury_1	512992	8966700	235	705	89	275	**17,0**	223	**-5,0**
Samoylovitch_1	518092	9047154	267	454	102	289	**8,2**	264	**-1,1**
Simony_1	501600	8904048	188	377	52	236	**25,7**	172	**-8,1**
Simony_3	499786	8891447	184	640	58	226	**23.8**	174	**-4.7**
Tyndall_2	581555	8938802	396	2150	196	353	**-10,9**	408	**3,1**
Tyndall_3	558992	8934430	241	396	146	253	**5,2**	237	**-1,5**
Tyndall_4	544475	8950346	757	1519	313	922	**21,8**	706	**-6,7**
Tyndall_6	559866	8970110	329	737	92	317	**-3,5**	335	**2,1**
Tyndall_7	575083	8975183	346	627	187	406	**17,4**	335	**-3,0**
Vostok_1	561661	9001031	297	414	185	320	**7,7**	289	**-2,7**
Vostok_2	575999	8994078	115	243	61	129	**12,2**	112	**-3,1**
Vostok_3	562830	8985155	79	306	13	113	**42,9**	72	**-9,2**

https://doi.org/10.5194/essd-2022-44
Preprint. Discussion started: 17 February 2022

Open Access Earth System Science Data Discussions

Table B3. Severnaya Zemlya: statistics for time series of Sentinel-1 velocity 2015-2021.

Name	Long.	Lat.	Mean Year	Max Year	Min Year	Mean Summer	Percent Summer	Mean Winter	Percent Winter
Academy Sciences 1	463595	8946216	449	783	329	509	**13,4**	428	**-4,7**
Academy Sciences 2	467049	8929805	1092	1347	968	1118	**2,4**	1076	**-1,4**
Academy Sciences 3	446085	8907872	302	522	164	363	**20,2**	277	**-8,5**
Academy Sciences 4	438899	8907977	1985	3909	1095	2122	**6,9**	1919	**-3,3**
Academy Sciences 5	434144	8905336	230	449	114	275	**19,9**	204	**-11,1**
Academy Sciences 6	419184	8899208	1239	1854	1026	1341	**8,2**	1189	**-4,0**
Academy Sciences 7	374753	8916934	220	564	113	262	**19,2**	199	**-9,3**
Karpinsky 1	481328	8860608	225	576	68	286	**27,4**	196	**-12,6**
Karpinsky 2	487193	8862193	541	1133	213	650	**20,1**	488	**-9,8**
Karpinsky 3	503943	8804018	176	302	82	199	**13,1**	166	**-5,5**
Rusanov 1	457762	8893341	201	473	60	240	**19,5**	194	**-3,3**
Rusanov 2	480060	8885389	80	136	50	82	**2,7**	79	**-1,2**
Rusanov 3	472768	8864412	309	517	161	325	**5,2**	300	**-2,6**
Rusanov 4	466164	8861665	157	320	63	156	**-1,0**	160	**1,6**
University 1	511895	8783252	117	452	17	120	**3,1**	118	**1,4**
University 2	515118	8756727	134	219	34	142	**6,2**	130	**-3,1**
Vavilov	406736	8808844	2062	4586	424	2117	**2,6**	2021	**-2,0**

https://doi.org/10.5194/essd-2022-44
Preprint. Discussion started: 17 February 2022

Open Access Earth System Science Data Discussions

Table B4. Svalbard: statistics for time series of Sentinel-1 velocity 2015-2021.

Name	Long.	Lat.	Mean Year	Max Year	Min Year	Mean Summer	Percent Summer	Mean Winter	Percent Winter
Austre_Torellbreen	502580	8565444	442	835	80	466	**5.5**	429	**-2.9**
Basin 3	711428	8832955	2650	4110	1645	2787	**5.2**	2538	**-4.2**
Bodleybreen	627736	8868785	510	915	70	440	**-13.6**	534	**4.8**
Borebreen	478403	8706253	168	347	14	213	**26.7**	153	**-9.4**
Dahlbreen	444663	8725316	246	382	125	234	**-4.8**	250	**1.7**
Davisbreen	556124	8574936	192	410	31	220	**14.5**	178	**-7.0**
Duvebreen	667145	8913229	183	389	19	171	**-6.6**	186	**1.6**
Fjortende_Julibreen	436246	8784037	301	705	45	273	**-9.2**	309	**2.7**
Frazerbreen	606529	8862302	182	300	41	163	**-10.2**	189	**3.7**
Hansbreen	516088	8549357	202	1208	8	156	**-22.7**	219	**8.4**
Hinlopenbreen	583959	8784448	305	1109	3	447	**46.2**	266	**-12.8**
Hornbreen	542711	8553974	402	1246	105	461	**14.5**	377	**-6.3**
Idabreen	445555	8837424	199	501	30	133	**-33.1**	227	**14.2**
Idunbreen	592453	8858413	334	649	34	343	**2.7**	326	**-2.6**
Kongsbreen	450119	8766388	396	683	152	326	**-17.6**	425	**7.4**
Konowbreen	456867	8724324	258	459	36	241	**-6.9**	265	**2.6**
Kronebreen	448626	8756665	1042	1760	491	1165	**11.8**	1004	**-3.7**
Leighbreen	723112	8918854	653	1134	366	578	**-11.5**	682	**4.4**
Lilliehöökbreen_W	430572	8813106	446	705	179	389	**-12.7**	465	**4.3**
Monacobreen	449191	8827445	987	1905	80	950	**-3.7**	994	**0.7**
Muehlbacherbreen	522618	8558392	318	593	30	235	**-26.0**	351	**10.3**
Negribreen	590175	8725568	3148	8663	165	3668	**16.5**	2905	**-7.7**
Olsokbreen	537713	8515419	532	1340	29	638	**19.9**	502	**-5.6**
Petermannbreen	584480	8716920	546	1087	240	594	**8.9**	521	**-4.4**
Rijpbreen	626849	8899792	573	860	342	577	**0.8**	566	**-1.2**
Schweigaardbreen	686848	8923033	643	944	198	623	**-3.2**	645	**0.4**
Seligerbreen	446360	8828938	341	1061	122	276	**-19.1**	369	**8.3**
Smeerenburgbreen	431070	8840351	249	426	95	210	**-15.8**	265	**6.4**
Svalisbreen	543289	8546268	369	1217	53	337	**-8.7**	380	**3.0**
Sveabreen	483328	8718988	461	975	93	370	**-19.8**	499	**8.2**

https://doi.org/10.5194/essd-2022-44
Preprint. Discussion started: 17 February 2022

Open Access Earth System Science Data Discussions

690 **Appendix C. Glacier's time series.**

Figure C1. Novaya Zemlya: time series of Sentinel-1 velocity 2015-2021.

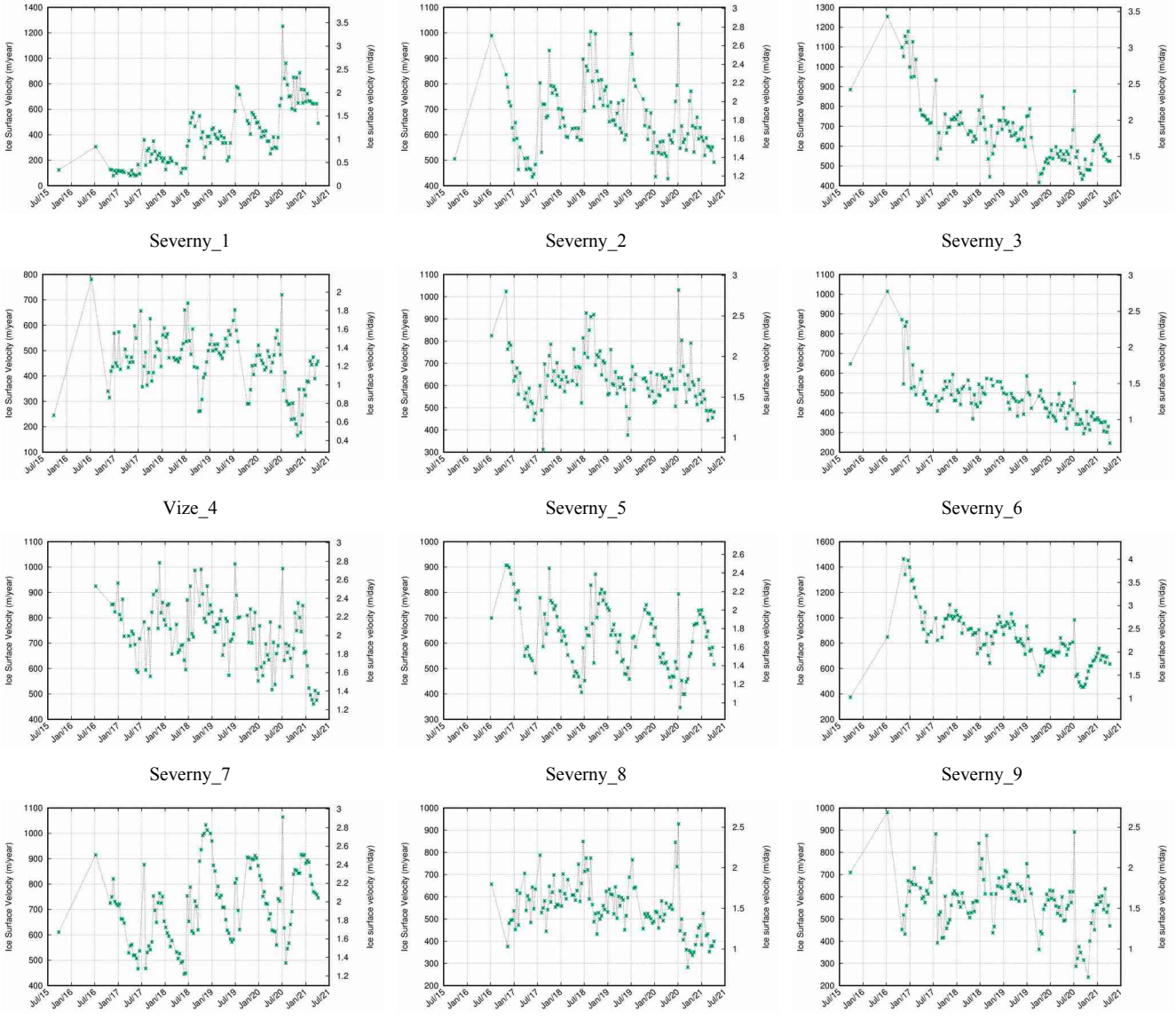

https://doi.org/10.5194/essd-2022-44
Preprint. Discussion started: 17 February 2022

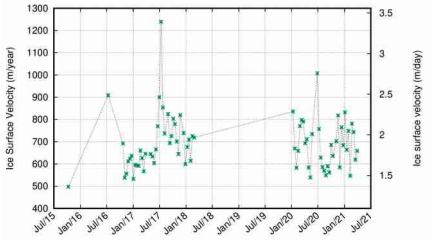

Krivosheina_13

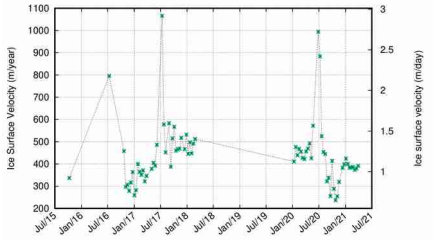

Vilkitskiy_14

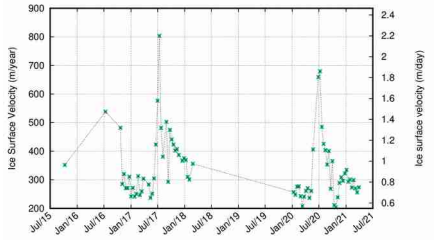

Severny_15

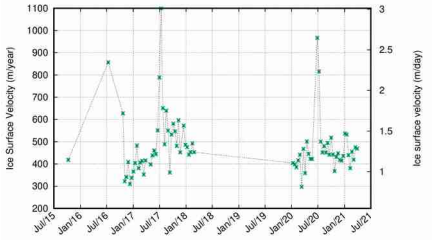

Nordenskiold_16

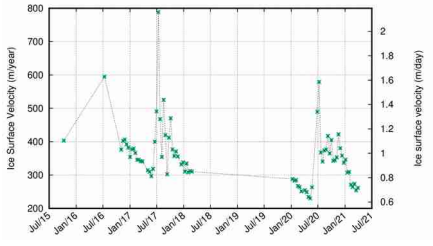

Glazov_17

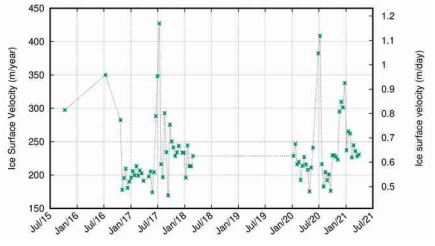

Nizkiy_18

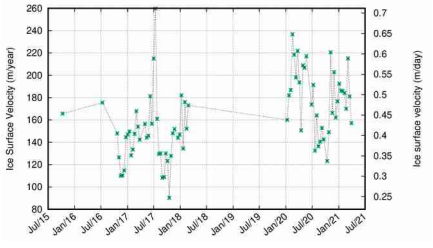

Severny_92

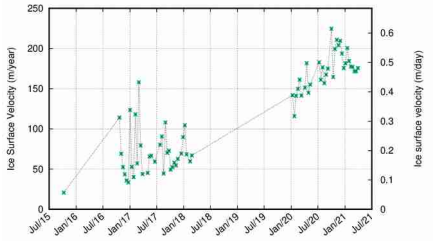

Severny_93

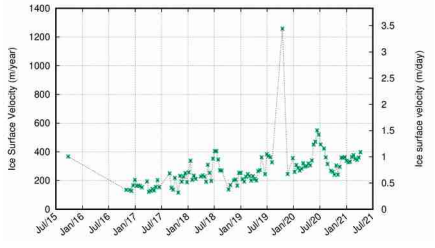

Severny_94

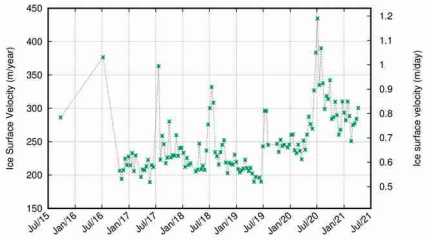

Vylki_Shury_95

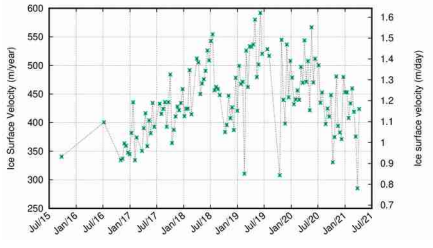

Severny_96

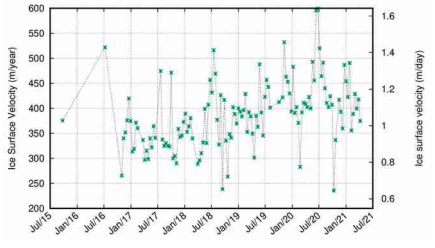

Moshchnyy_97

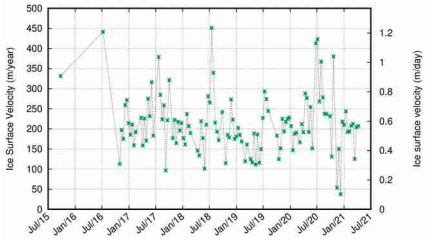

Severny_98

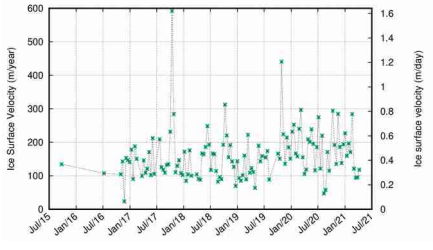

Severny_99

https://doi.org/10.5194/essd-2022-44
Preprint. Discussion started: 17 February 2022

Open Access Earth System Science Data Discussions

Figure C2. Franz-Josef-Land: time series of Sentinel-1 velocity 2015-2021.

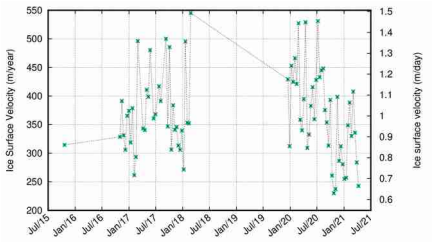

Brousilov_1

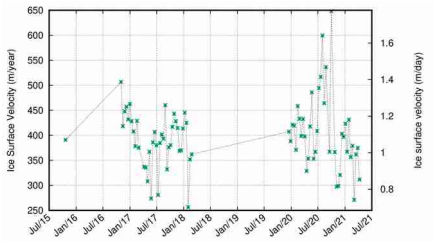

Brousilov_2

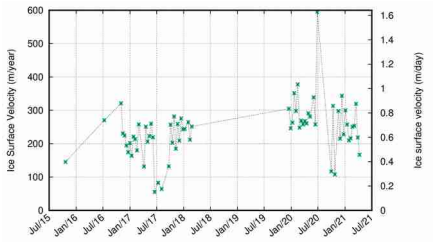

Brousilov_3

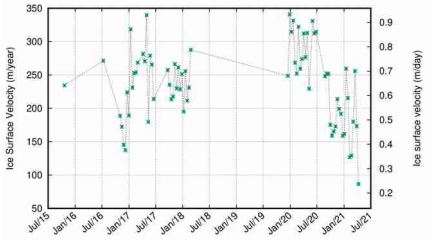

Brousilov_4

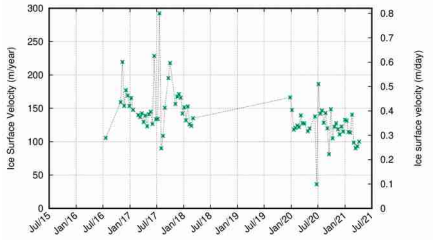

Champ

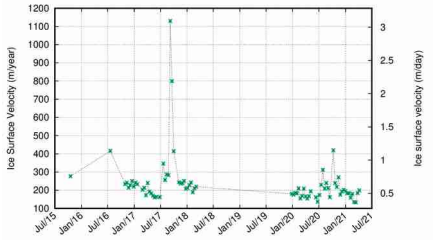

Chernysheva

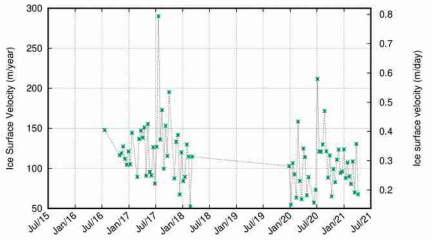

Forbes

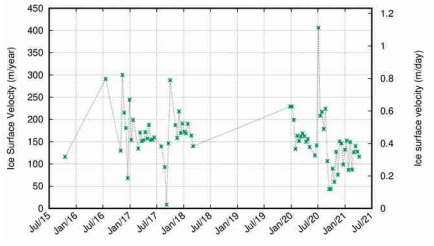

Luigi

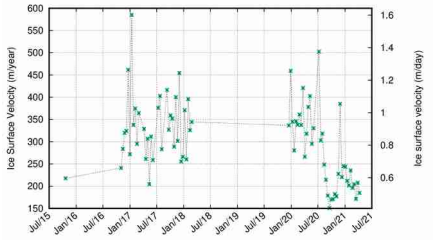

Moon_4

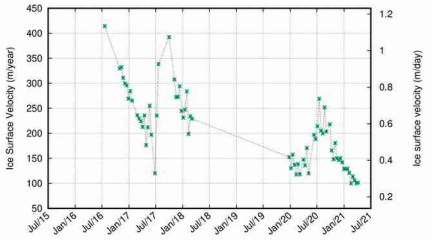

Moscow_1

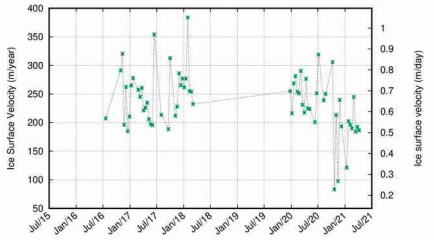

Moscow_2

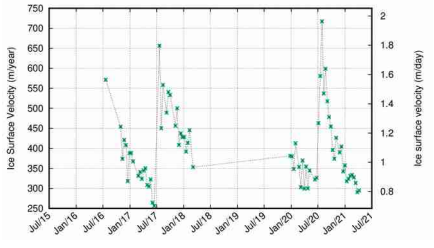

Moscow_3

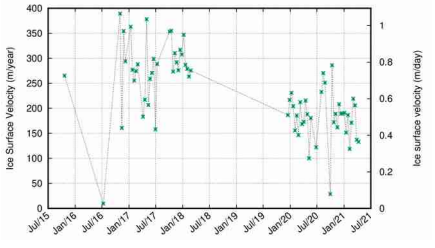

Northbrook_2

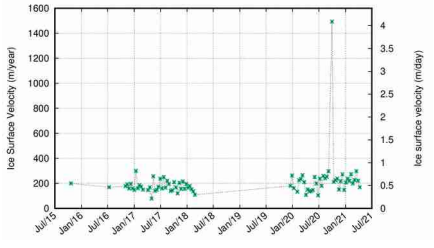

Rudolph_Island_1

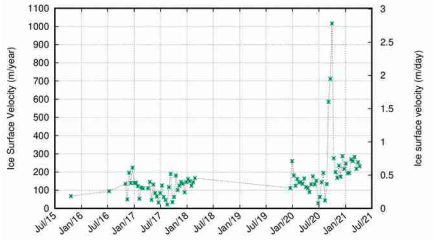

Rudolph_Island_2

https://doi.org/10.5194/essd-2022-44
Preprint. Discussion started: 17 February 2022

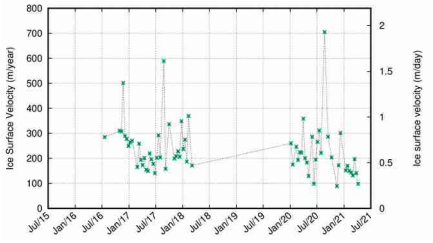

Salisbury_1

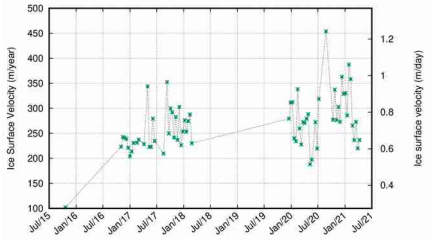

SamoylovitchIceCap_1

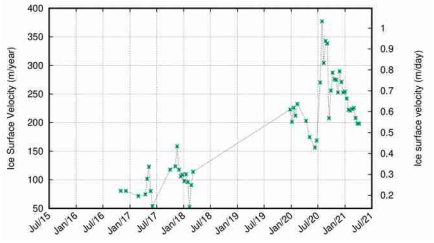

Simony_1

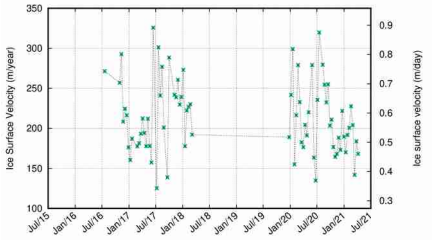

Simony_3

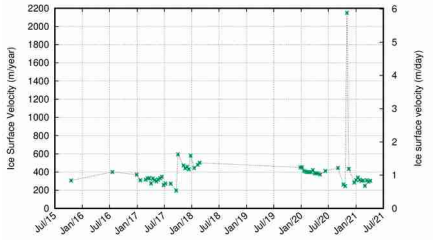

TyndallIceCap_2

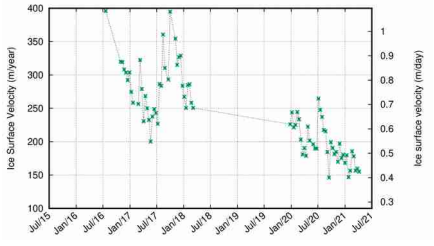

TyndallIceCap_3

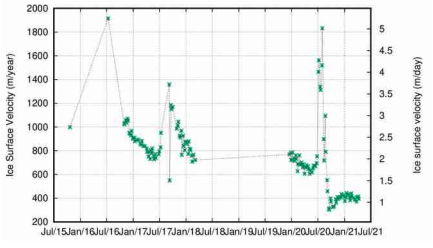

TyndallIceCap_4

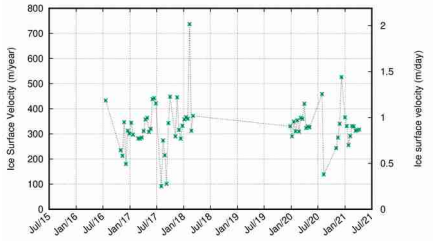

TyndallIceCap_6

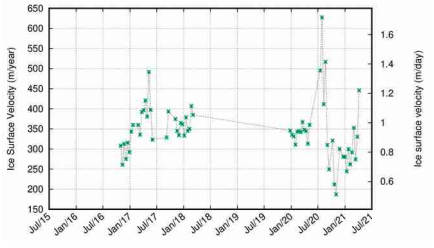

TyndallIceCap_7

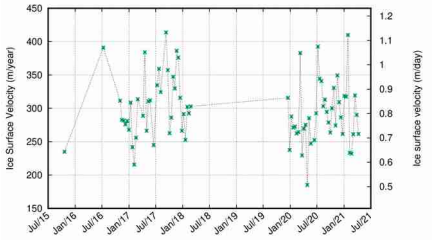

Vostok-1IceCap_1

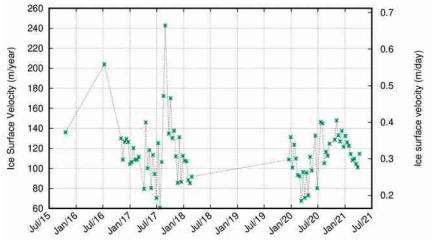

Vostok-1IceCap_2

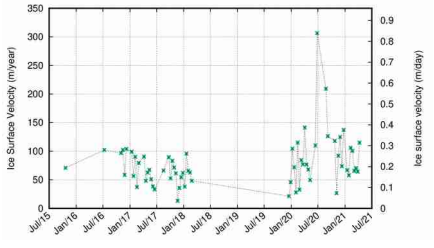

Vostok-1IceCap_3

695

https://doi.org/10.5194/essd-2022-44
Preprint. Discussion started: 17 February 2022

Open Access Earth System Science Data Discussions

Figure C3. Severnaya Zemlya: time series of Sentinel-1 velocity 2015-2021.

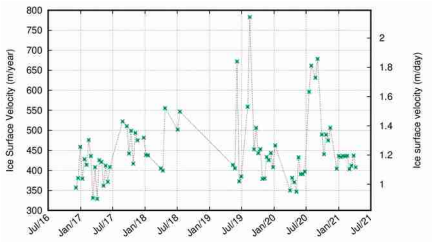

Academy_of_Sciences_1

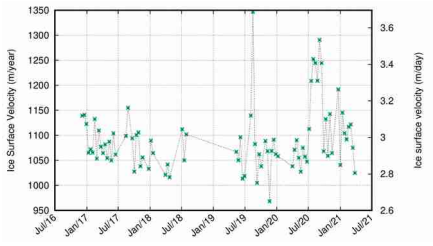

Academy_of_Sciences_2

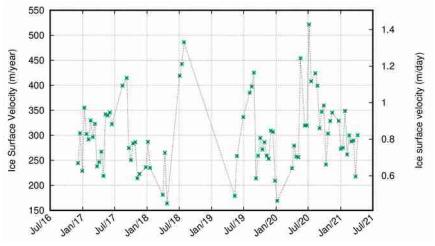

Academy_of_Sciences_3

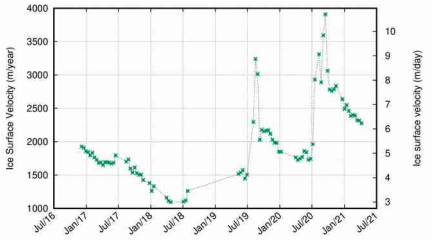

Academy_of_Sciences_4

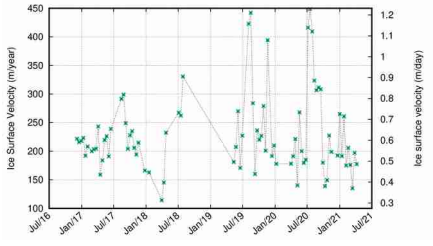

Academy_of_Sciences_5

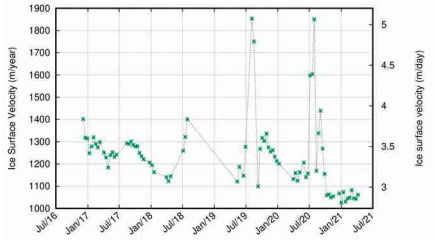

Academy_of_Sciences_6

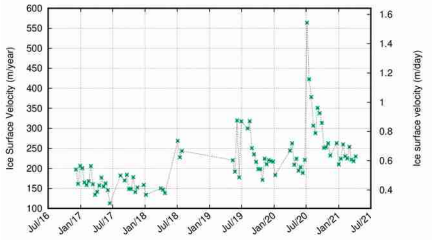

Academy_of_Sciences_7

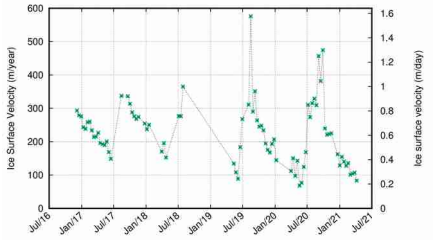

Karpinsky_Ice_Cap_1

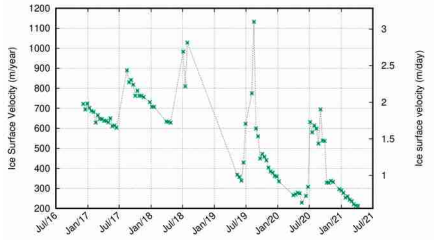

Karpinsky_Ice_Cap_2

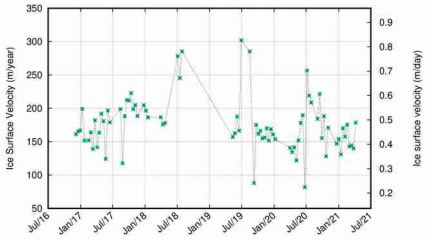

Karpinsky_Ice_Cap_3

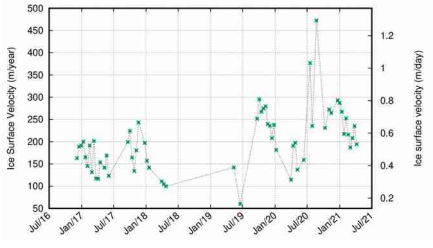

Rusanov_Ice_Cap_1

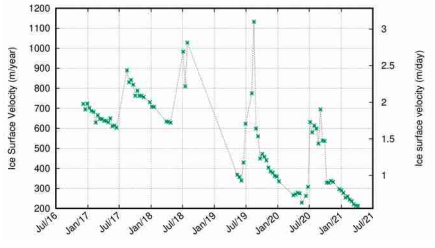

Rusanov_Ice_Cap_2

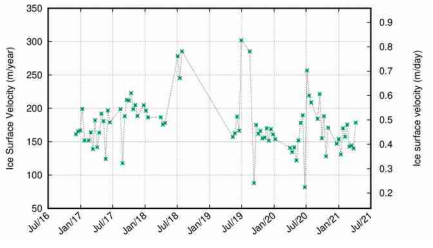

Rusanov_Ice_Cap_3

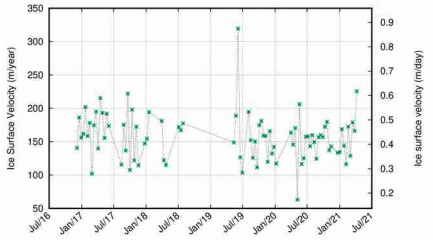

Rusanov_Ice_Cap_4

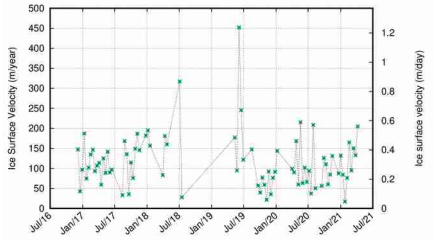

University_Ice_Cap_1

https://doi.org/10.5194/essd-2022-44
Preprint. Discussion started: 17 February 2022

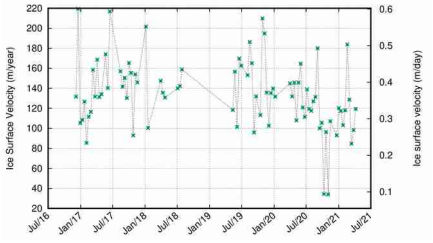

University_Ice_Cap_2

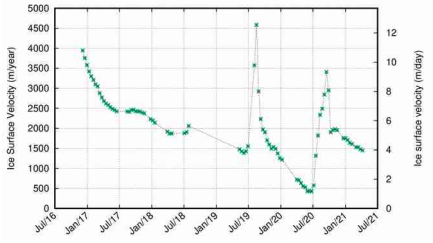

Vavilov_T77

https://doi.org/10.5194/essd-2022-44
Preprint. Discussion started: 17 February 2022

Open Access Earth System Science Data Discussions

Figure C4. Svalbard: time series of Sentinel-1 velocity 2015-2021.

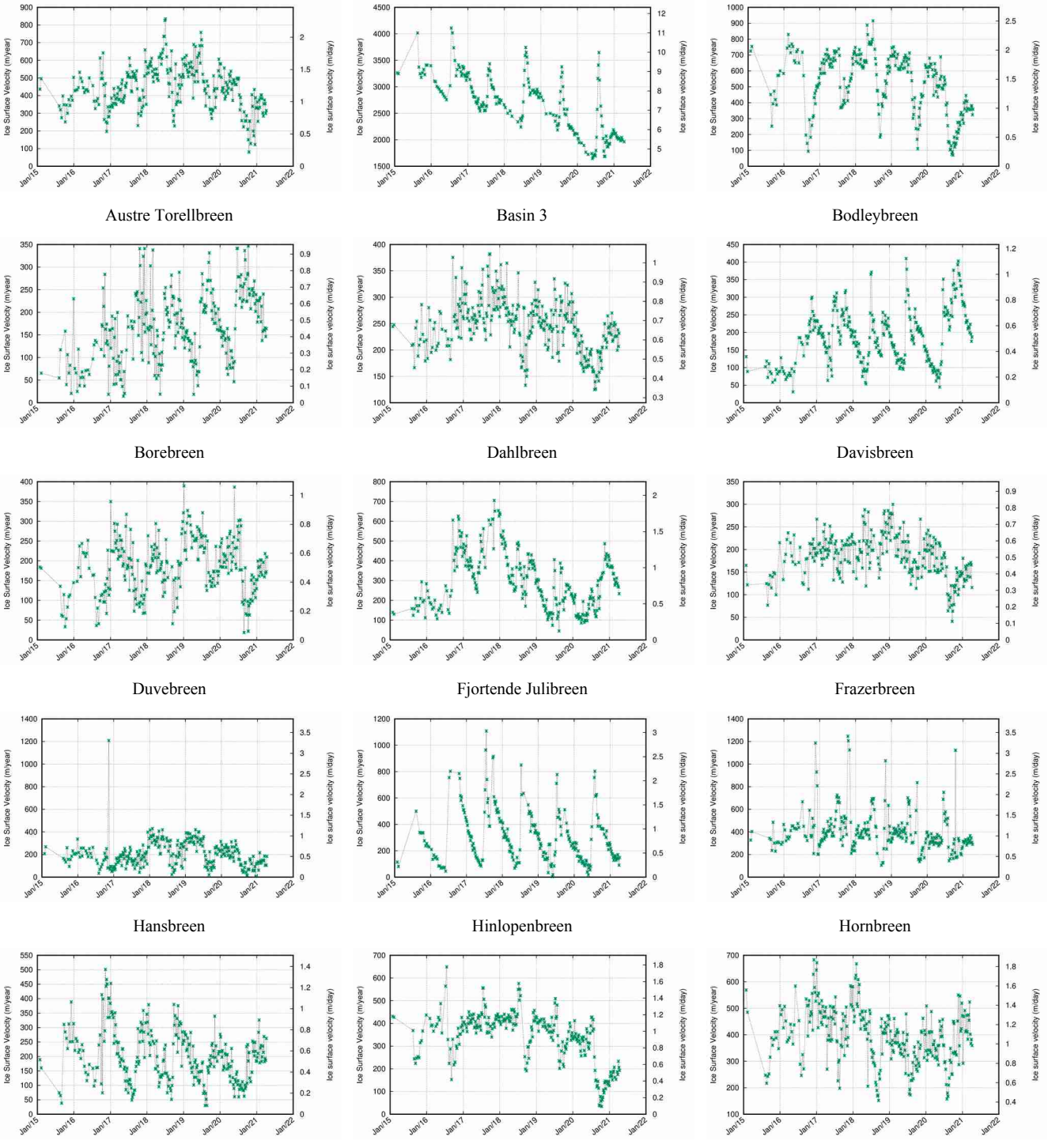

https://doi.org/10.5194/essd-2022-44
Preprint. Discussion started: 17 February 2022

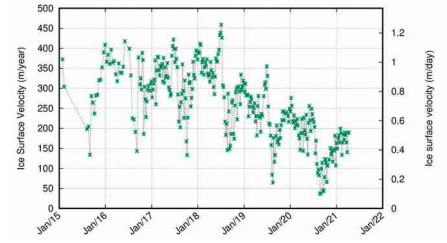

Konowbreen

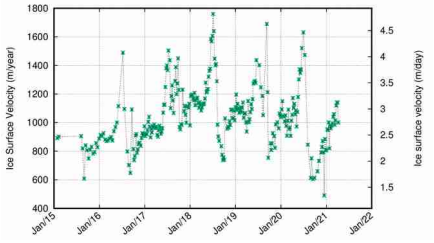

Kronebreen

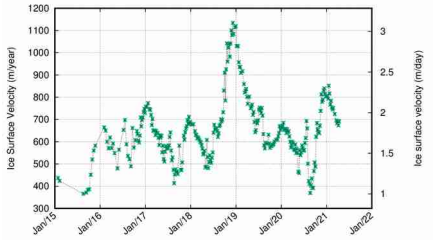

Leighbreen

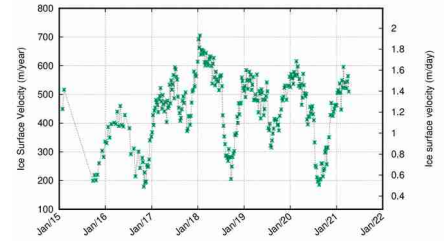

Lilliehöökbreen West

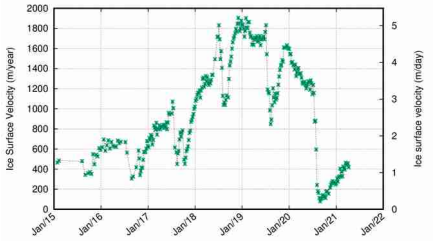

Monacobreen

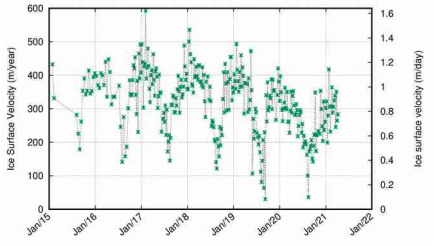

Muehlbacherbreen

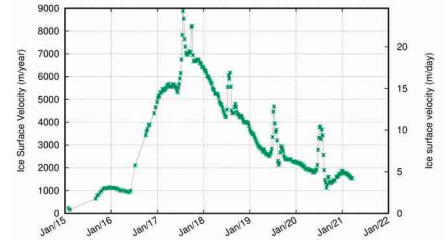

Negribreen

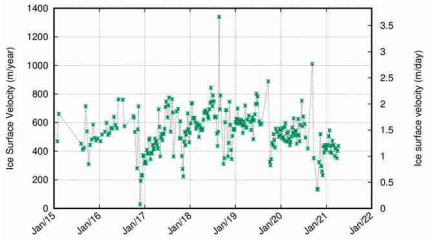

Olsokbreen

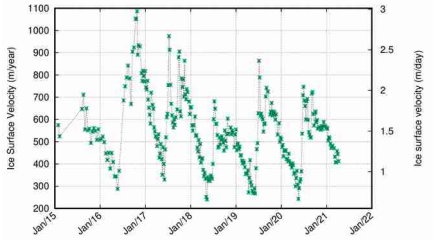

Petermannbreen

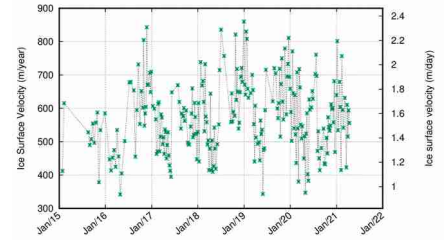

Rijpbreen

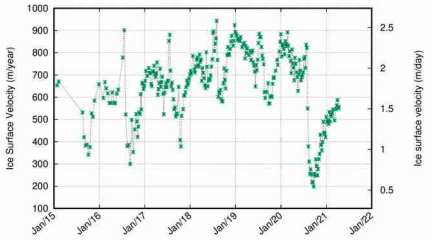

Schweigaardbreen

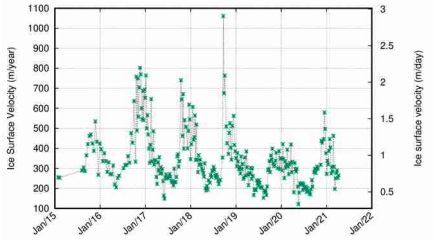

Seligerbreen

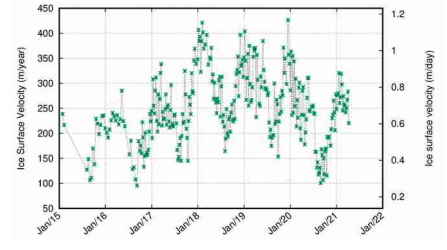

Smeerenburgbreen

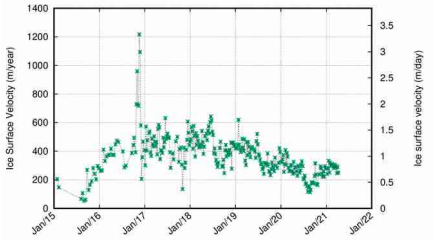

Svalisbreen

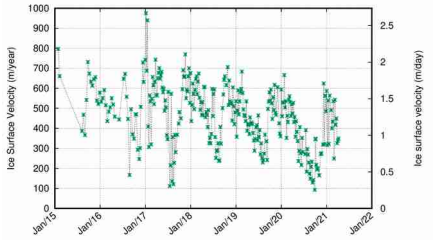

Sveabreen

700